Tornado and Tornado Dynamics

<u>Readings:</u>

Markowski and Richardson book section 10.1.

Klemp (1987) Dynamics of Tornadic Thunderstorms (handout)

Bluestein Vol II. Section 3.4.8.

Rotunno, R., 1986: Tornadoes and tornadogenesis. In: P. Ray (Editor), *Mesoscale Meteorology and Forecasting*. AMS, Boston, 414-436.

Davie-Jones, Robert, R. J. Trapp, and H. B. Bluestein, 2001, Tornadoes and Tornadic Storms, In: C. A. Doswell (Editor), Severe Convective Storms, AMS, 167-222.

Houze Sections 8.6-8.

<u>Definition</u>: tornado, n. A rotating column of air usually accompanied by a funnel-shaped downward extension of a cumulonimbus cloud and having, ..[winds] whirling destructively at speeds of up to 300 miles per hour. (American Heritage Dictionary of the English Language)

This definition reflects a fundamental property of the tornado: it occurs in association with a thunderstorm.

Definition in Markowski and Richardson book: Tornadoes are violently rotating columns of air, usually associated with a swirling cloud of debris or dust near the ground and a funnel-shaped cloud extending downward from the base of the parent cumulonimbus updraft.

Wind Speed inside tornadoes

Horizontal wind speeds in tornadoes can be as high as **100-150 m/s**.

There is some theoretical evidence that **even stronger upward vertical velocities** can occur near center of a tornado, near the ground.

The **maximum possible tornadic wind speed** is a function not only of the **hydrostatic-pressure deficit** owing to latent-heat release in the updraft, which is a function of the CAPE, but also to the **dynamic-pressure deficit**, which is a function of the character of the wind field itself, especially in the surface boundary layer.

Fujita Scale (F-scale)

T. Fujita developed a wind speed scale to assess tornado damage and estimate the maximum tornado intensity. Called the F-scale, it was designed to link the Beaufort wind scale with the Mach scale.

A Beaufort force of 12 (minimal hurricane force winds) was equal to F1, and F12 was equal to Mach 1 (the speed of sound). The minimum wind speed (v_{min} in mph) of any F-scale range (F) was $v_{min} = 14.1(F + 2)^{3/2}$.

The Fujita Scale of Tornado Intensity

F-Scale Number	Intensity Phrase	Wind Speed	Type of Damage Done
F0	Gale tornado	40-72 mph (18-32m/s)	Some damage to chimneys; breaks branches off trees; pushes over shallow-rooted trees; damages sign boards.
F1	Moderate tornado	73-112 mph (33-50m/s)	The lower limit is the beginning of hurricane wind speed; peels surface off roofs; mobile homes pushed off foundations or overturned; moving autos pushed off the roads; attached garages may be destroyed.
F2	Significant tornado	113-157 mph (51-71m/s)	Considerable damage. Roofs torn off frame houses; mobile homes demolished; boxcars pushed over; large trees snapped or uprooted; light object missiles generated.
F3	Severe tornado	158-206 mph (72-93m/s)	Roof and some walls torn off well constructed houses; trains overturned; most trees in forest uprooted
F4	Devastating tornado	207-260 mph (94-117m/s)	Well-constructed houses leveled; structures with weak foundations blown off some distance; cars thrown and large missiles generated.
F5	Incredible tornado	261-318 mph (118-143m/s)	Strong frame houses lifted off foundations and carried considerable distances to disintegrate; automobile sized missiles fly through the air in excess of 100 meters; trees debarked; steel reinforced concrete structures badly damaged.
F6	Inconceivable tornado	319-379 mph (144-170m/s)	These winds are very unlikely. The small area of damage they might produce would probably not be recognizable along with the mess produced by F4 and F5 wind that would surround the F6 winds. Missiles, such as cars and refrigerators would do serious secondary damage that could not be directly identified as F6 damage. If this level is ever achieved, evidence for it might only be found in some manner of ground swirl pattern, for it may never be identifiable through engineering studies

Enhanced Fujita scale (EF-scale)

In 2007, the enhanced Fujita scale (EF-scale) was adopted in the United States. It was designed to improve the accuracy of wind speed estimates derived from observed damage, in part, by attempting to account for the quality of construction.

Tornadoes rated EF0–EF1, EF2–EF3, and EF4–EF5 are referred to as weak, strong, and violent tornadoes, respectively.

EF0 (65–85 mph 3-s gusts) tornado damages include damage to chimneys, broken tree branches, and damage to sign boards.

EF1 (86–110 mph 3-s gusts) tornado damages include destroyed garages or barns and peeled-off roofs.

An EF2 (111–135 mph 3-s gusts) tornado may tear roofs off frame houses, obliterate mobile homes, and snap or uproot large trees.

EF3 (136–165 mph 3-s gusts) tornadoes destroy interior walls of well-constructed homes.

EF4 (166–200 mph 3-s gusts) tornadoes are capable of completely leveling a well-built home.

An EF5 (>200 mph 3-s gusts) tornado strips clean the foundation of a well-built structure and is capable of throwing automobiles over 100 m.

Any estimation of tornado strength based on damage is error-prone for a number of reasons, including variations in the duration of extreme winds and debris loading within a tornado, not to mention the fact that many tornadoes do not strike man-made structures. Furthermore, EF-scale (and F-scale) ratings are based on the maximum damage observed. Even the most intense tornado that one might expect to be able to observe, an EF5, typically only contains EF5 winds within a region occupying less than 10% of the total path area.

References:

WSEC, 2006: A recommendation for an enhanced Fujita scale (EF-scale). Texas Tech University Wind Science and Engineering Center Rep., 95 pp. [Available online at www.depts.ttu.edu/weweb/pubs/fscale/efscale.pdf.]

Roger Edwards, James G. LaDue, John T. Ferree, Kevin Scharfenberg, Chris Maier, and William L. Coulbourne, 2013: Tornado Intensity Estimation: Past, Present, and Future. *Bull. Amer. Meteor. Soc.*, **94**, 641–653. doi: http://dx.doi.org/10.1175/BAMS-D-11-00006.1

Relationship between severity of observed thunderstorms and the CAPE and vertical wind shear of the environments, as determined by proximity soundings.

Red dots indicate tornado reports. Grey dots indicate non-tornadic damaging wind and/or large hail reports. Black dots indicate non-severe thunderstorm reports. Adapted from a figure in Brooks et al. (2003).

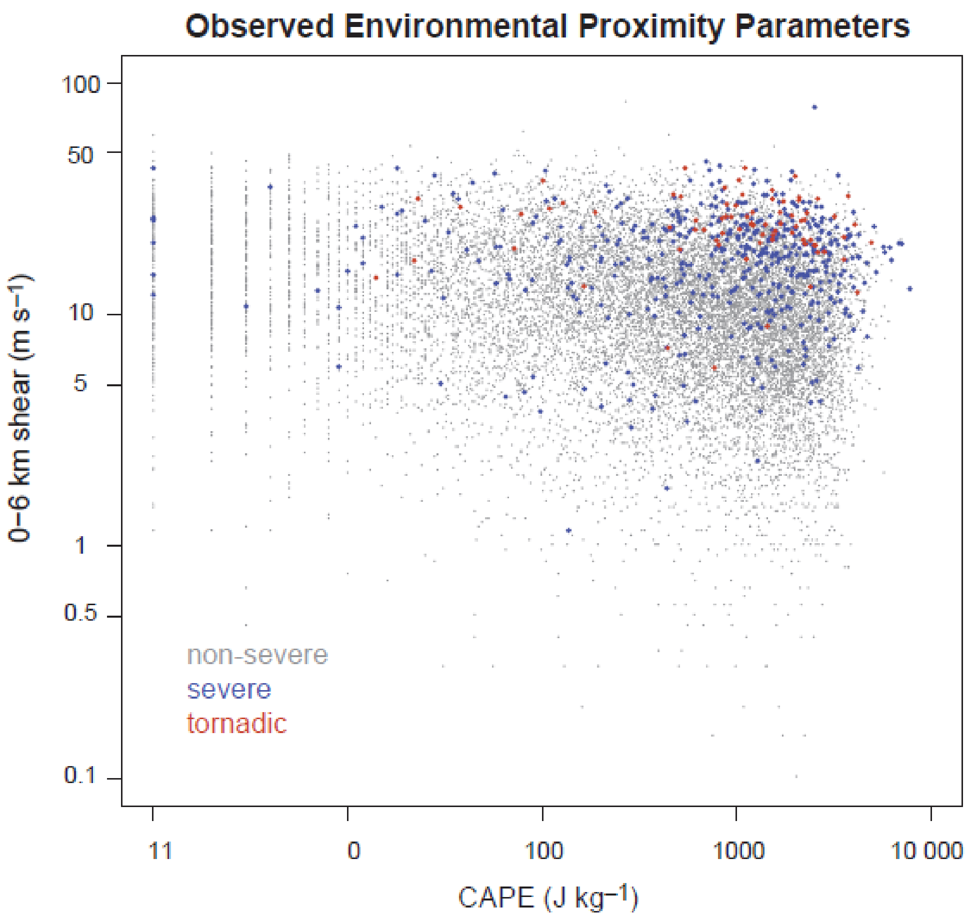

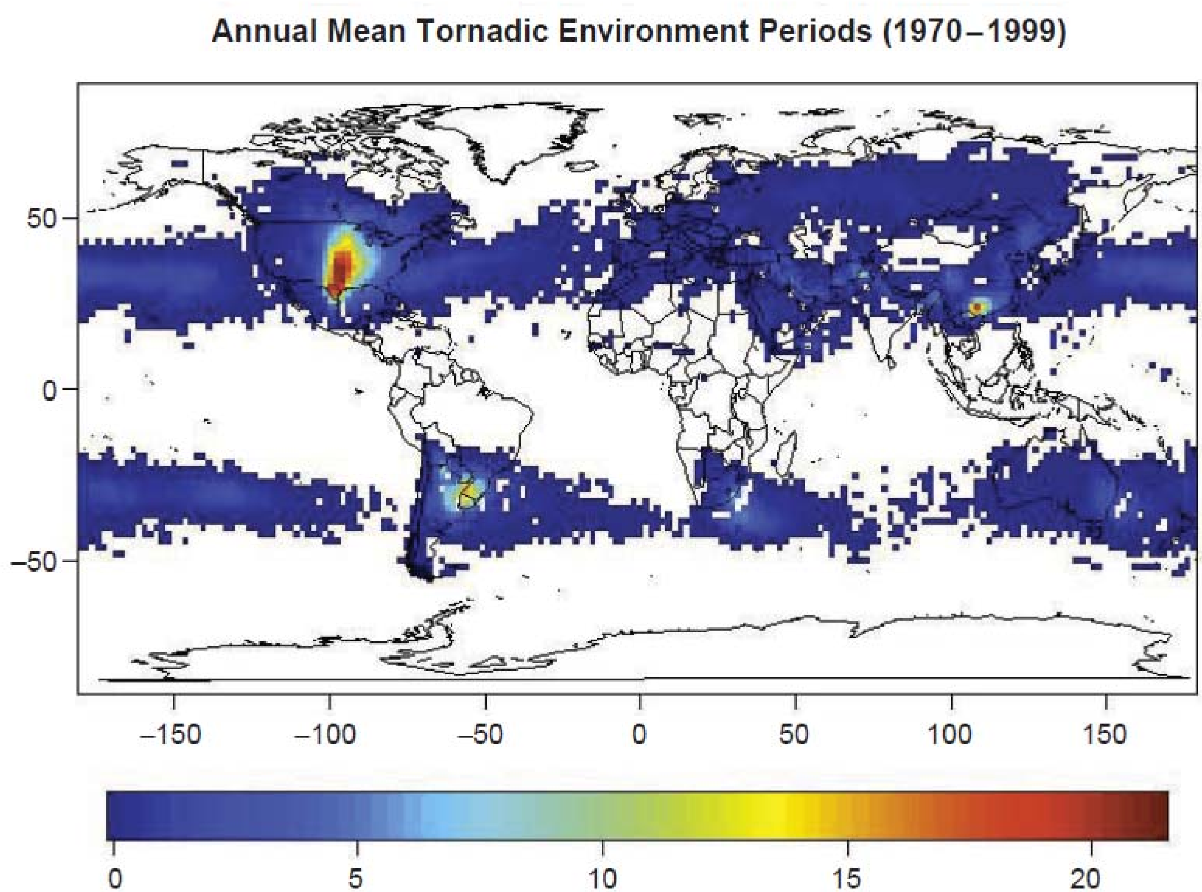

Average number of days per year having environments favorable for tornadic supercells were convection to form. Such conditions include the presence of strong shear over a deep tropospheric layer and CAPE (these are the conditions required for supercells), as well as strong low-level shear and high boundary layer relative humidity. The above *synthetic climatology* of tornadic supercell days, which is based on analyses obtained from the global reanalysis program, is shown instead of actual tornadic supercell or tornado reports because of the lack of reliable reports over the vast majority of the earth. (From Brooks *et al*. [2003].)

Tornado Climatology in the US

Tornadoes in the United States are reported most frequently in a band stretching from West and North Texas through Oklahoma, central and eastern Kansas, and into eastern Nebraska. This region is referred to as **tornado alley**.

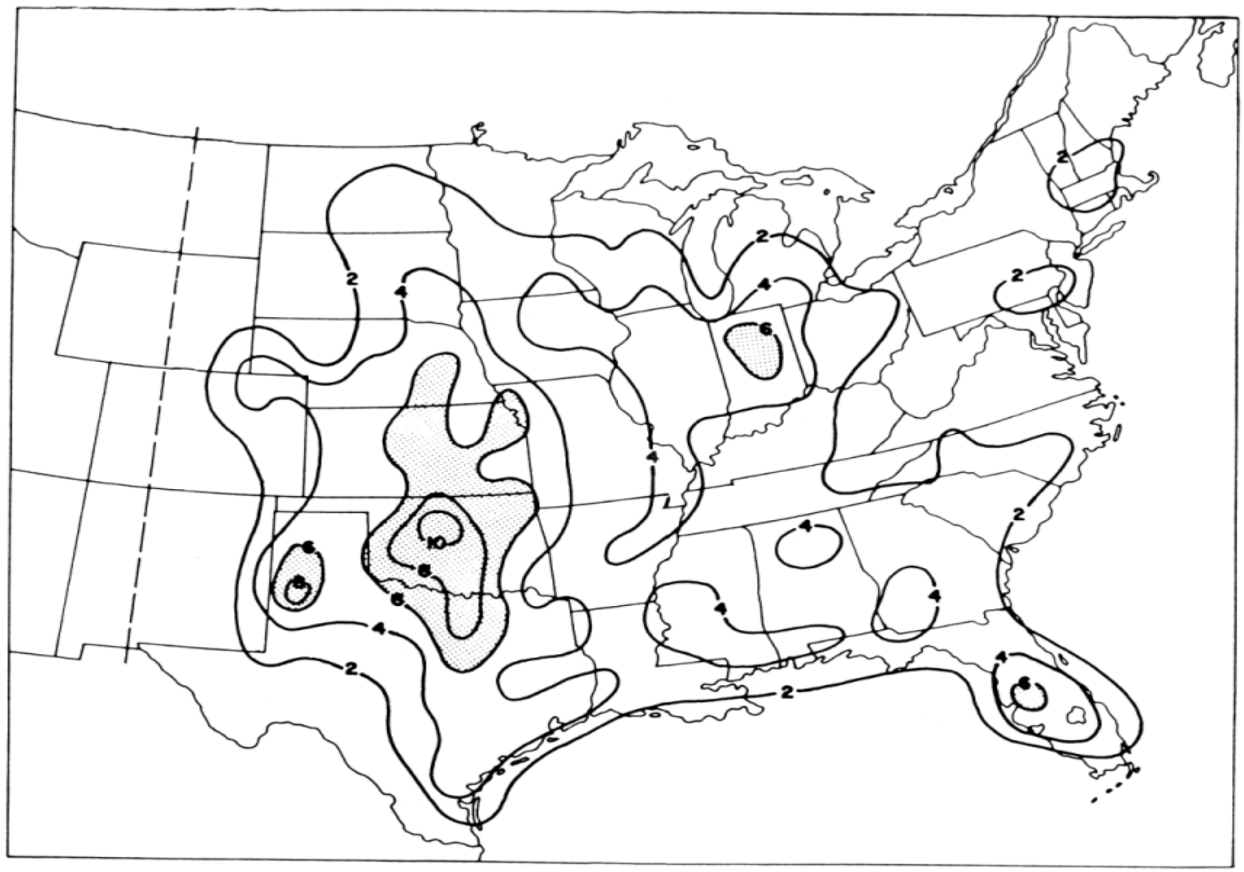

Figure 3.68 Frequency distribution of tornadoes (1950–1976) in the United States. Tornadoes per 2° latitude–longitude overlapping quadrilateral, normalized to 10,000 nm^2 area, per year (from Doswell, 1985; adapted from Kelly et al., 1978). (Courtesy of the American Meteorological Society)

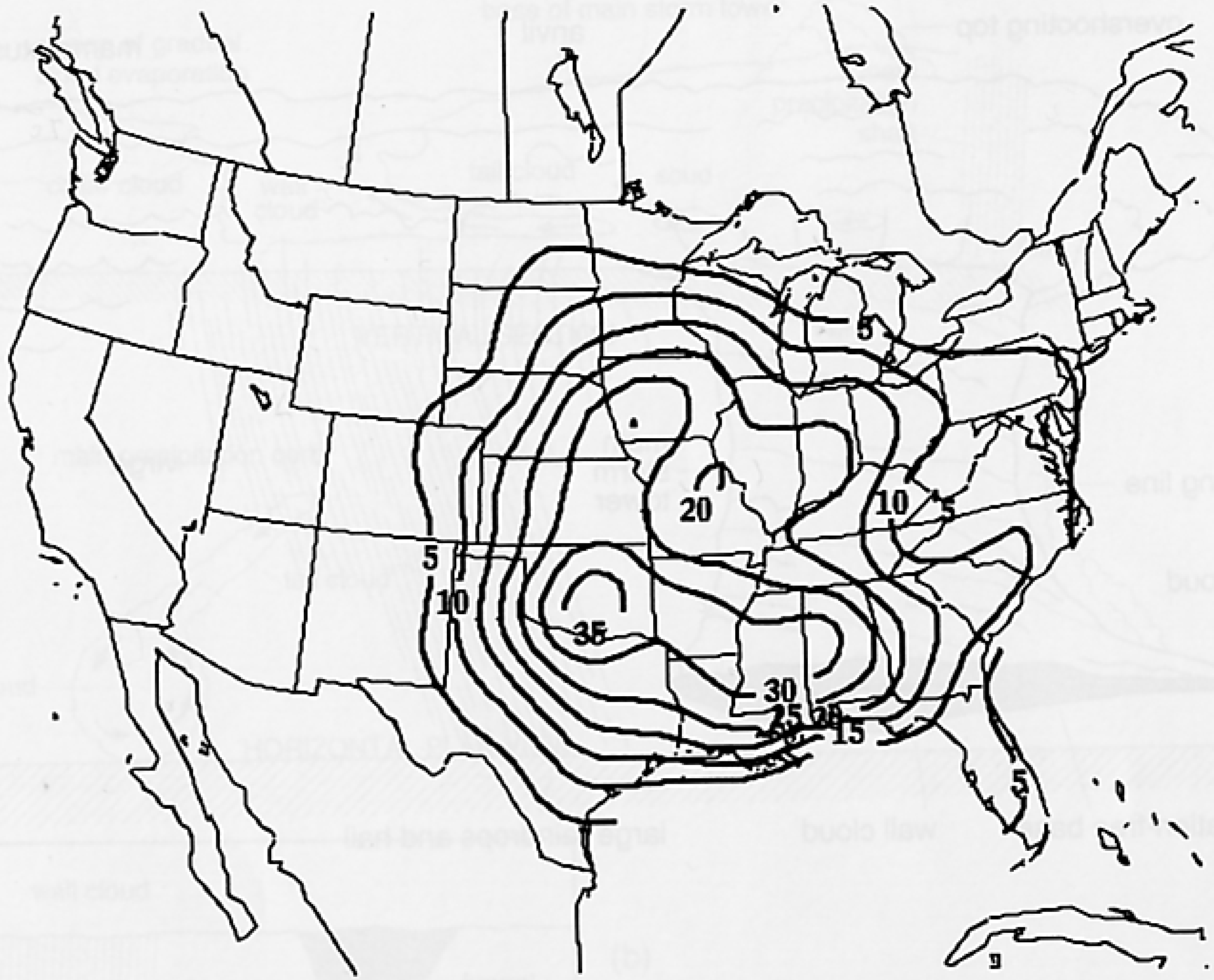

FIG. 5.5. Based on data from 1921 to 1995, the mean number of days per century of F2 intensity or greater tornado occurrence within 40km of a point in the United States (Concannon et al. 2000). Contour interval is 5 days, with minimum level equal to 5.

The **elevated terrain** to the west and southwest of the Great Plains and the Gulf of Mexico play important roles in producing soundings having high amounts of CAPE.

The sloping terrain is partially responsible for the **lee trough and low-level jet**, the latter which **advects the Gulf marine layer northward**, while warm dry air caps the moist layer.

The ubiquitous **dryline and fronts approaching from the north and northwest** are frequent locations of storm formation.

Most tornadoes occur during the **late afternoon and evening hours** in the late spring. This suggests that **solar heating plays an important role** in producing a potentially unstable environment for tornadic storm formation during the afternoon.

Major outbreaks occur primarily during the spring, when strong disturbances in the middle and upper troposphere promote regions of strong **lifting** and an environment of strong **vertical shear** and high values of **CAPE**.

Tornadic **activity begins along the Gulf States in late winter, and migrates northward,** so that summer activity is highest in the Northern Plains.

Environments for tornado outbreaks in the United States have been produced **as far east as the East Coast**.

Tornado outbreaks in late spring and early summer are often associated with short waves moving through northwesterly flow aloft, as a ridge is built up to the west and a trough is ensconced to the east.

In spring, outbreaks usually occur in southwesterly flow aloft, downstream from major troughs.

Relation of tornadoes to supercell storms

Although not all supercell storms produce tornadoes, most of the intense tornadoes are generated by them.

In a radar study of Oklahoma storms during 1971-1975, for example, Burgess (1976) found that 62% of the 37 storms that exhibited strong storm-scale rotation developed tornadoes while none occurred in storms which did not rotate.

=

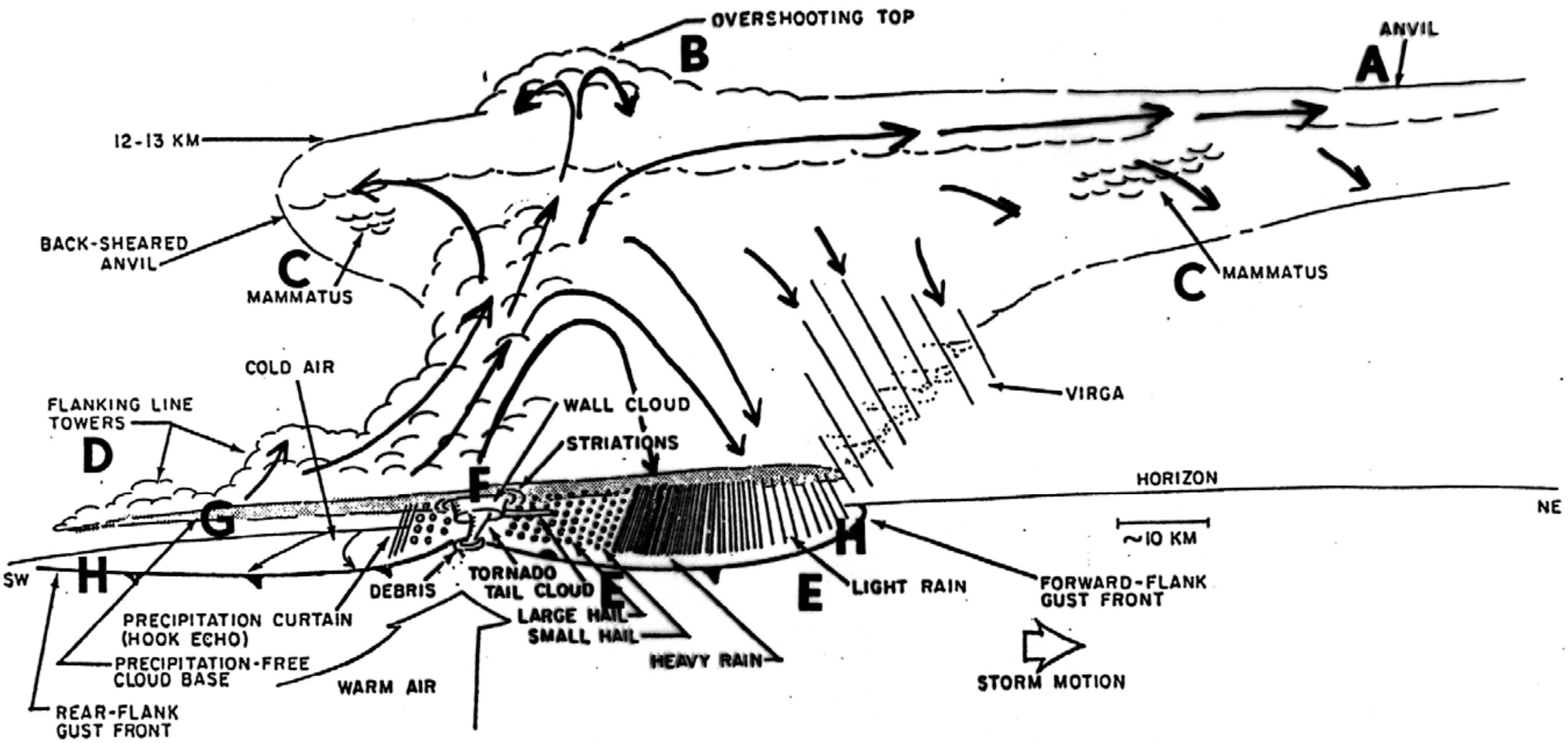

Tornadogenesis

Intensification of mesoclone rotation

Figure 12 illustrates schematically the flow structure within a numerically simulated supercell evolving in a unidirectional wind shear at a time when the low-level rotation is intensifying rapidly.

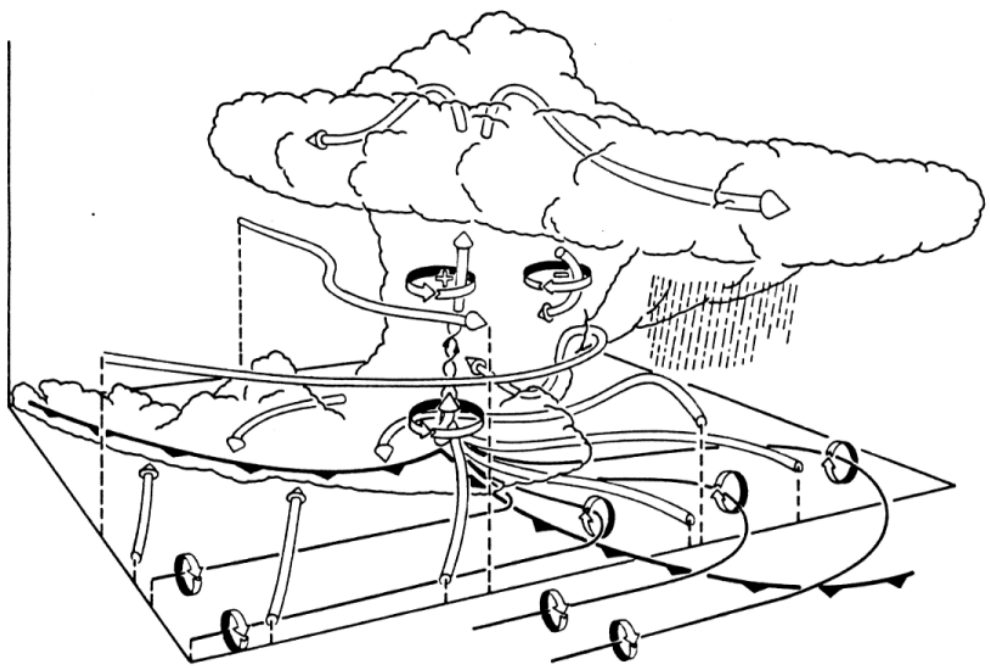

Figure 12 Three-dimensional schematic view of a numerically simulated supercell thunderstorm at a stage when the low-level rotation is intensifying. The storm is evolving in westerly environmental wind shear and is viewed from the southeast. The cylindrical arrows depict the flow in and around the storm. The thin lines show the low-level vortex lines, with the sense of rotation indicated by the circular-ribbon arrows. The heavy barbed line marks the boundary of the cold air beneath the storm.

Baroclinic generation of horizontal vorticity along the forward flank gust front (FFGF) can significantly enhance the horizontal vorticity of the inflow feeding the updraft.

This **horizontal vorticity is then tilted into the vertical** and strongly stretched as the inflow enters the low-level updraft.

To see how this situation arises, notice that in the evolving storm, precipitation is swept around to the northern side of the cyclonically rotating storm. As it falls to the north and northeast of the updraft, evaporation cools the low-level air. With time, this cold pool of air advances progressively into the path of the low-level inflow to the storm. **A significant portion of the inflow can be approaching along the boundary of this cold air pool**. The horizontal temperature gradients thus baroclinically generate horizontal vorticity that is nearly parallel to the inflowing streamlines. This process generates horizontal vorticity that is several times the magnitude of the mean shear vorticity and that is more favorably oriented to be tilted into vertical cyclonic vorticity.

Since the environmental shear is westerly, the horizontal vortex lines embedded in the shear are oriented south-north with the sense of rotation as indicated in the undisturbed region southeast of the storm in Figure 12. As these vortex lines penetrate the low-level pool of cold air, they turn rapidly toward the center of convergence and are swept into the updraft.

However, the tilting of horizontal vorticity into the vertical and the subsequent intensification of rotation due to stretching cannot explain the intensification of rotation near ground, because the tilted vortex tubes cannot intercept the ground and the vertical stretching is strongest above the ground (see Davis-Jones et al 2001).

Generation of large vertical vorticity at ground

- Tornadogenesis requires that large vertical vorticity arises at the ground.
- If no prior vertical vorticity exists near the ground, then vorticity stretching doesn't work.
- Tilting by an updraft is not effective at producing vertical vorticity near the surface because air is rising away from the surface as horizontal vorticity is tilted into the vertical.
- If downdraft does the tilting, then vertical vorticity created can be advected toward the surface, where it can subsequently be stretched to form a tornado.
- For these reasons, a downdraft is needed for tornadogenesis when preexisting rotation is absent near the ground.
- Furthermore, once a tornado is established, tilting of surface-layer horizontal vorticity by the extreme vertical velocity gradient associated with the tornado updraft itself probably contributes to the near-ground vertical vorticity in a significant way.
- However, such abrupt upward turning of streamlines, strong pressure gradients, and large vertical velocities are not present next to the ground prior to tornadogenesis; therefore, tilting by an updraft alone cannot be invoked to explain the amplification of near-ground vertical vorticity that results in tornadogenesis.

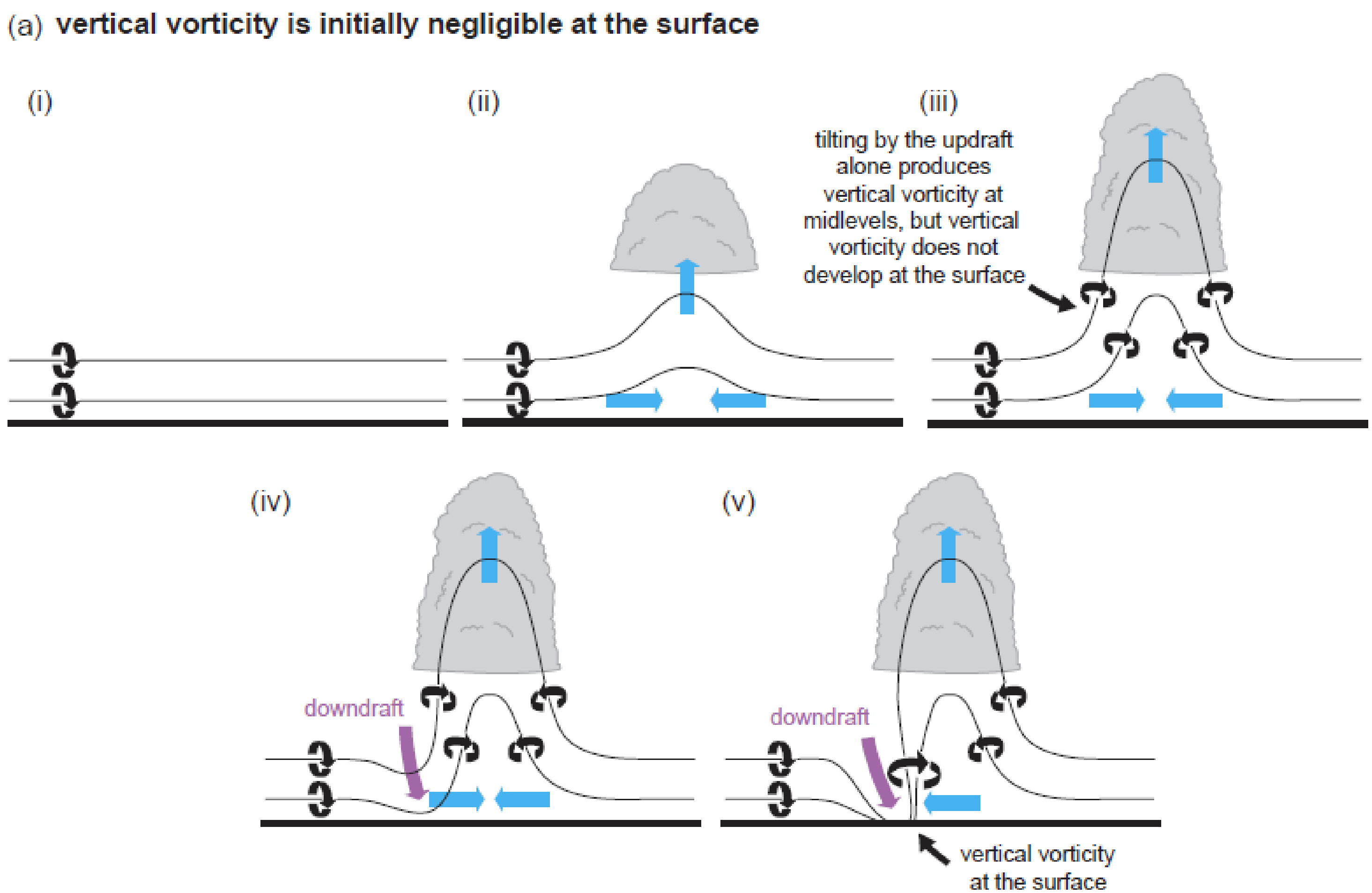

(a) Simple vortex line demonstration of why a downdraft is needed in order for significant vertical vorticity to develop at the ground beneath a thunderstorm in the absence of preexisting vertical vorticity at the surface. There is assumed to be no baroclinic vorticity generation; thus, the vortex lines are assumed to be frozen in the fluid.

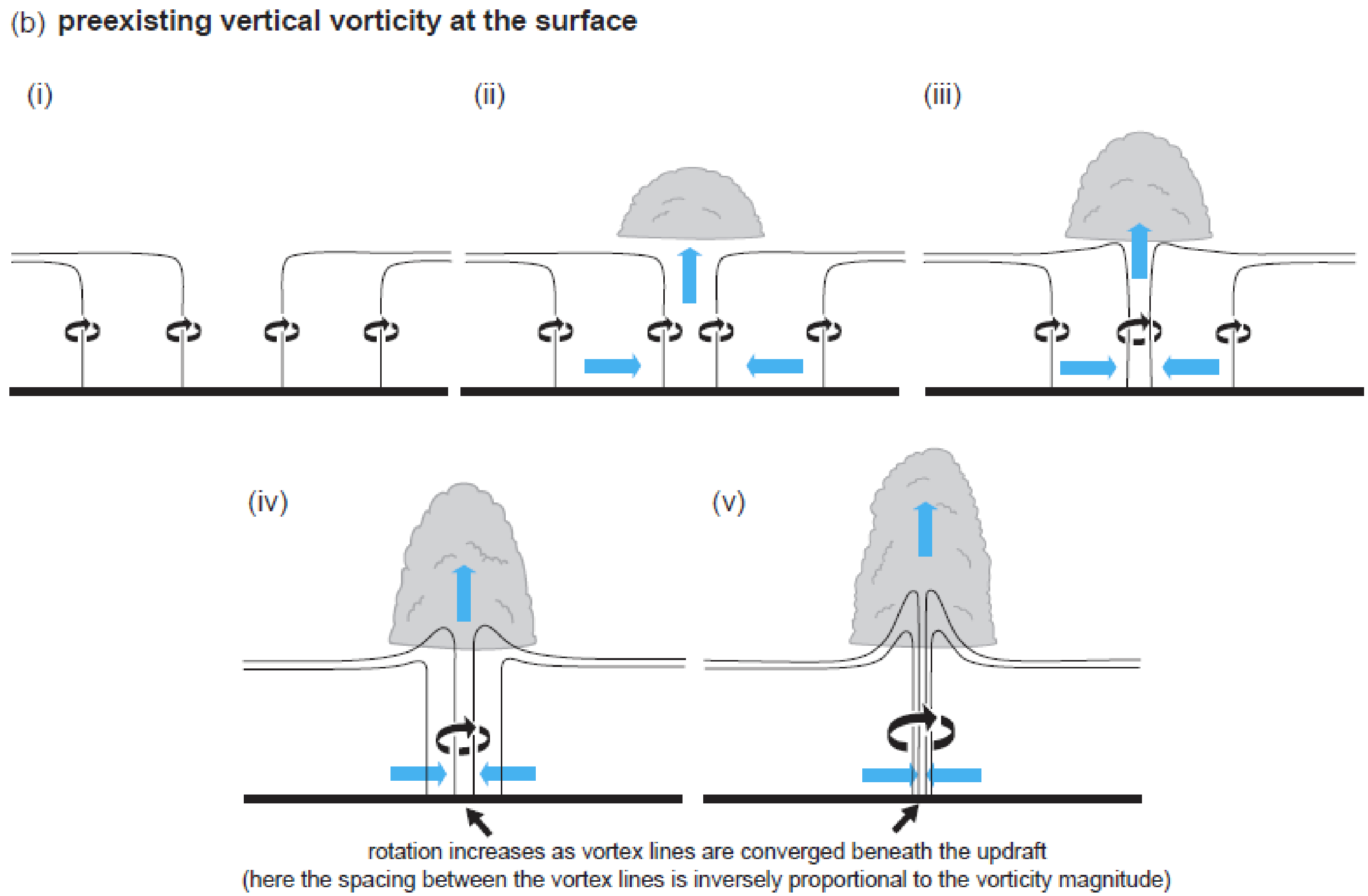

(b) Simple vortex line demonstration of how a tornado can arise from convergence alone, in the absence of a downdraft, when preexisting vertical vorticity is present at the ground.

Importance of downdrafts

The theoretical arguments for **the importance of downdrafts in tornadogenesis** have been verified in numerical simulations, and nearly countless observations exist of rear-flank downdrafts (RFDs), hook echoes, and **clear slots in close proximity to tornadoes** (Figure 10.4).

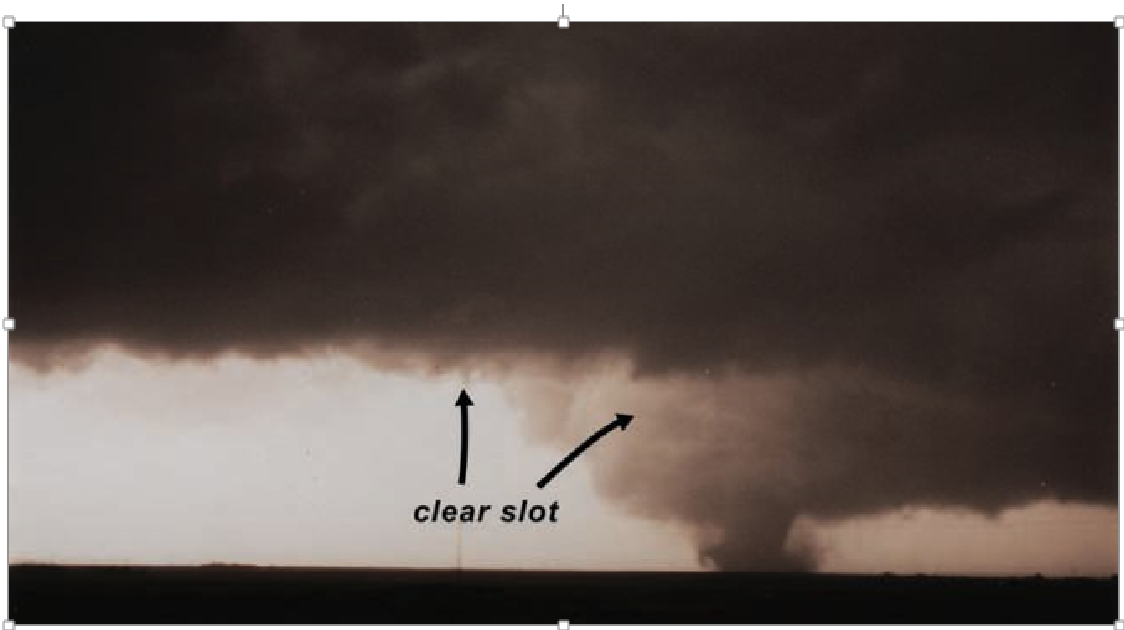

Figure 10.4 A clear slot like that shown above near the Dimmitt, TX, tornado on 2 June 1995 is a visual manifestation of sinking air, probably in what ought to be regarded as an *occlusion downdraft* (defined in Section 8.4 as a local, dynamically driven intensification of sinking motion within the larger-scale RFD). Photograph by Paul Markowski.

Furthermore, **trajectory analyses** in a limited number of observed supercells as well as in numerical simulations indicate that **at least some of the air entering the tornadoes** (or, in the case of simulations, intense vortices that appear tornadolike) **passes through the RFD prior to entering the tornado** (Figure 10.5).

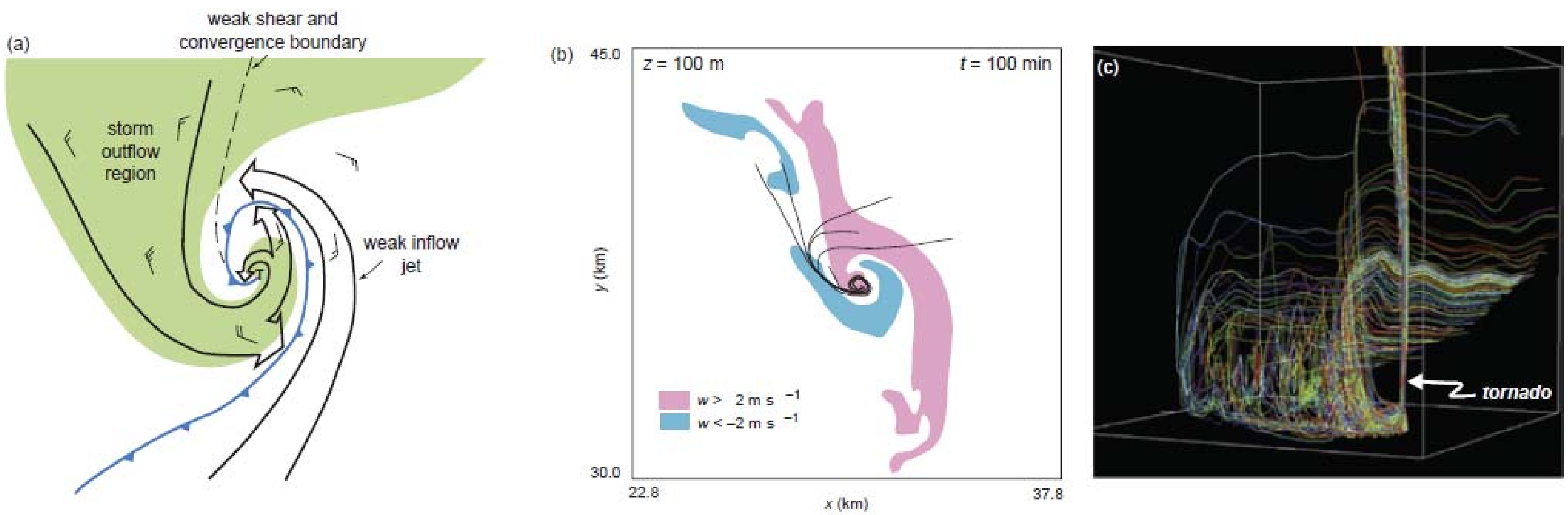

Figure 10.5 Observations and numerical simulations indicate that the air that enters tornadoes, tornado parent circulations, or nontornadic, near-ground circulations in supercells typically enters the circulations from the outflow air mass, rather than directly from the inflow. Such findings are consistent with the notion of downdrafts being important in the generation of rotation near the ground in supercells. (a) Trajectories in the RFD region composited from dual-Doppler observations of supercell thunderstorms (adapted from Brandes [1978]); (b) backward trajectories computed from the near-ground vertical vorticity maximum in a supercell simulation (adapted from Wicker and Wilhelmson [1995]); (c) a three-dimensional perspective from the southeast of trajectories entering a tornado that developed within a supercell simulation (from Xue [2004]; courtesy of Ming Xue).

Titling of baroclinically generated horizontal vortex lines into vertical

Analyses of vortex lines in the vicinity of low-level mesocyclones reveal that vortex lines form arches that join counter-rotating vortices (one of which is the cyclonic vortex associated with the tornado parent circulation) on opposite sides of the RFD (Figures 10.6 and 10.7), rather than vortex lines that are depressed downward as in Figure 10.3a, as would happen if a downdraft advects environmental vortex lines as material lines.

The arching vortex line structures are also consistent with the notion of a downdraft playing a fundamental role in the generation of rotation near the ground. In fact, the arching vortex line structure bears a striking resemblance to the structure of the vortex lines that pass through the line-end vortices of bow echoes (Figure 9.27).

In bow echoes baroclinically generated vortex lines within the outflow are lifted out of the outflow along the outflow's leading edge, leading to the counter-rotating, line-end vortices. It is tempting to wonder whether similar dynamics are at work in the RFD region of supercell thunderstorms — that is, a baroclinic process (Figure 10.8) rather than simply a redistribution of environmental vorticity (Figure 10.3a) —as is suggested by the vortex line configuration evident in Figure 10.6.

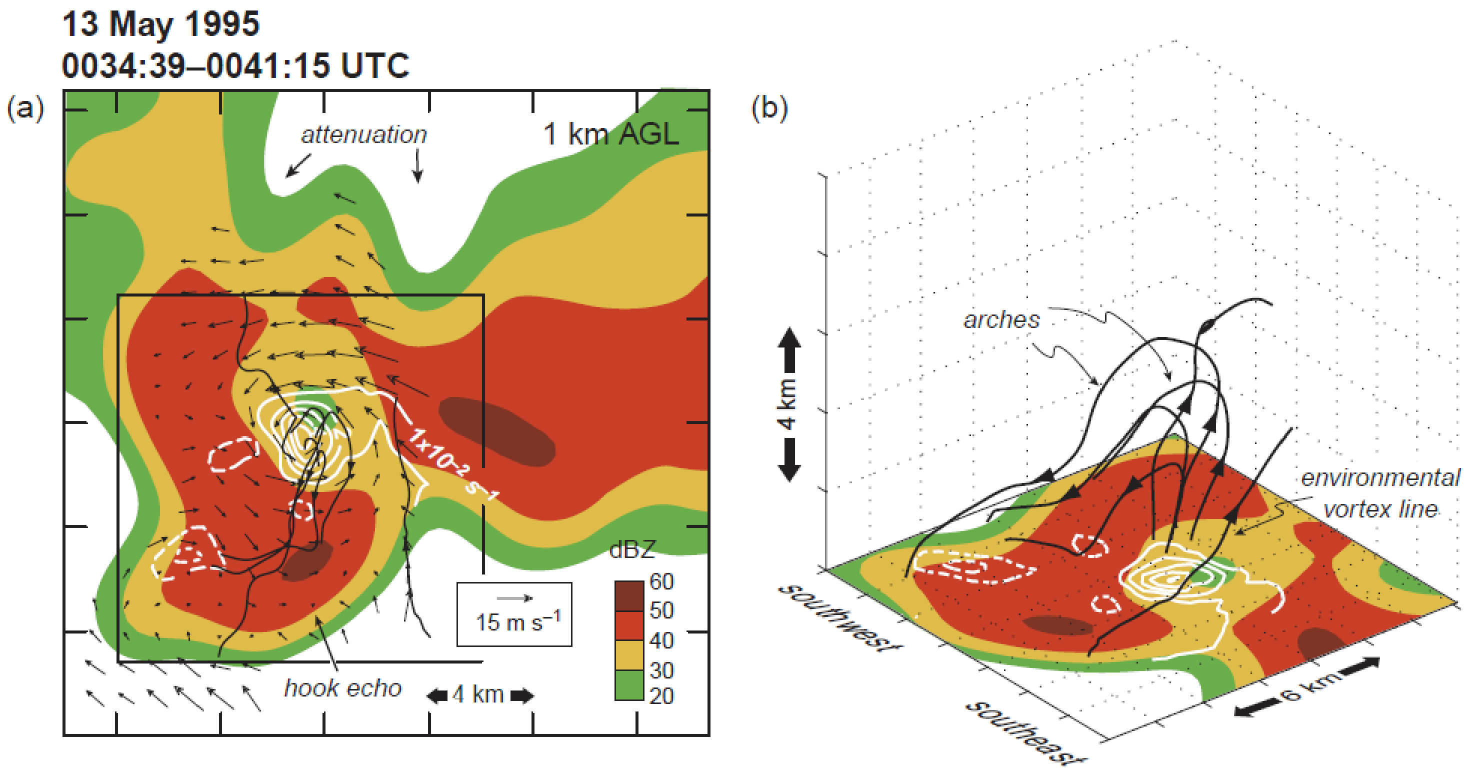

Figure 10.6 (a) Radar reflectivity factor (dBZ; shaded) at 1.0 km AGL at 0034:39–0041:15 UTC 13 May 1995. Dual-Doppler-derived, storm-relative wind vectors and vertical vorticity (white) contours (10^{-2} s^{-1} contour interval; the zero contour is suppressed and negative contours are dashed) at the same altitude are also overlaid, as are projections of select vortex lines (bold solid lines) onto the ground. The direction of the vorticity vector is indicated by the arrowheads. Five of the vortex lines pass through points centered on and surrounding the vertical vorticity maximum at 1.0 km. A sixth vortex line originates in the environment ahead of the gust front. The region enclosed by the square is shown in (b). (b) A three-dimensional perspective of the vortex lines emanating from the low-level mesocyclone center. For purposes of clarity, the reflectivity and vertical vorticity fields at 1.0 km AGL are displayed at the bottom of the three-dimensional domain. (Adapted from Markowski *et al*. [2008].)

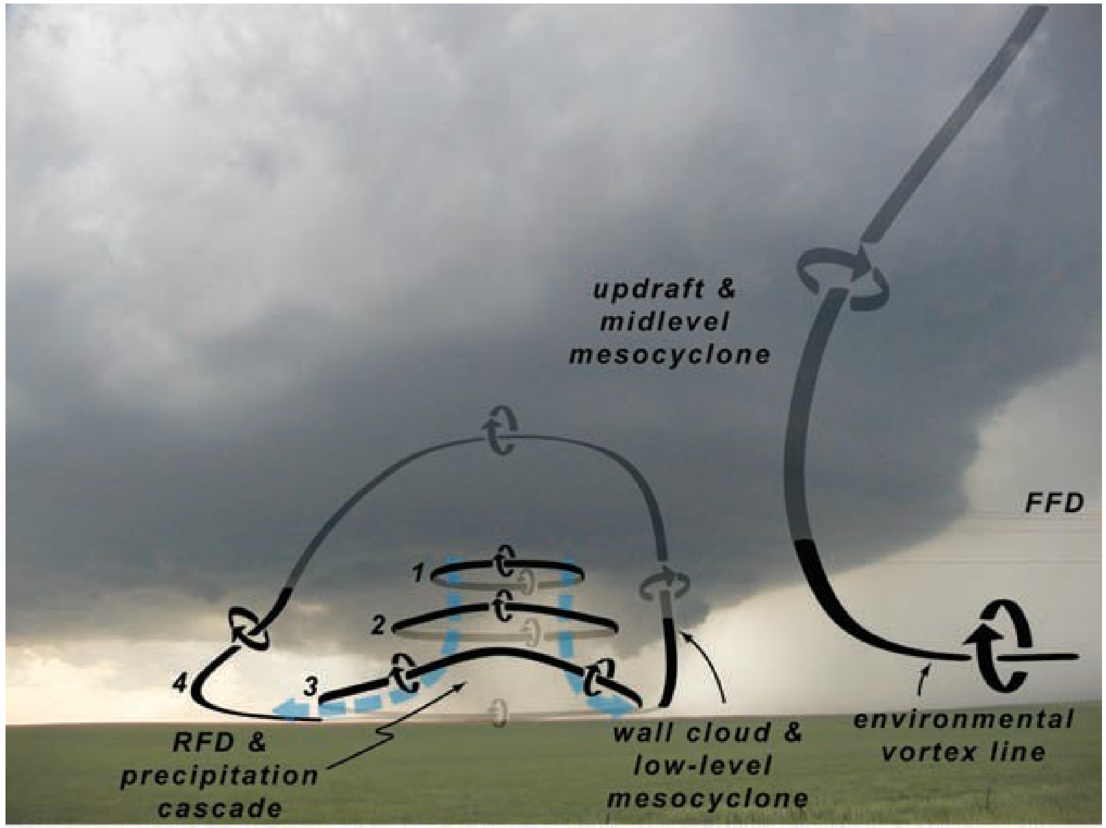

Figure 10.7 Idealized evolution of vortex rings and arches inferred from the sample of supercells analyzed by Markowski *et al*. [2008], superimposed on a photograph of a supercell thunderstorm (courtesy of Jim Marquis; the view is from the south). The numerals 1 – 4 can indicate either a single vortex line seen at four different times in a sequence, or four different vortex lines at a single time but in different stages of evolution. An environmental vortex line is also shown.

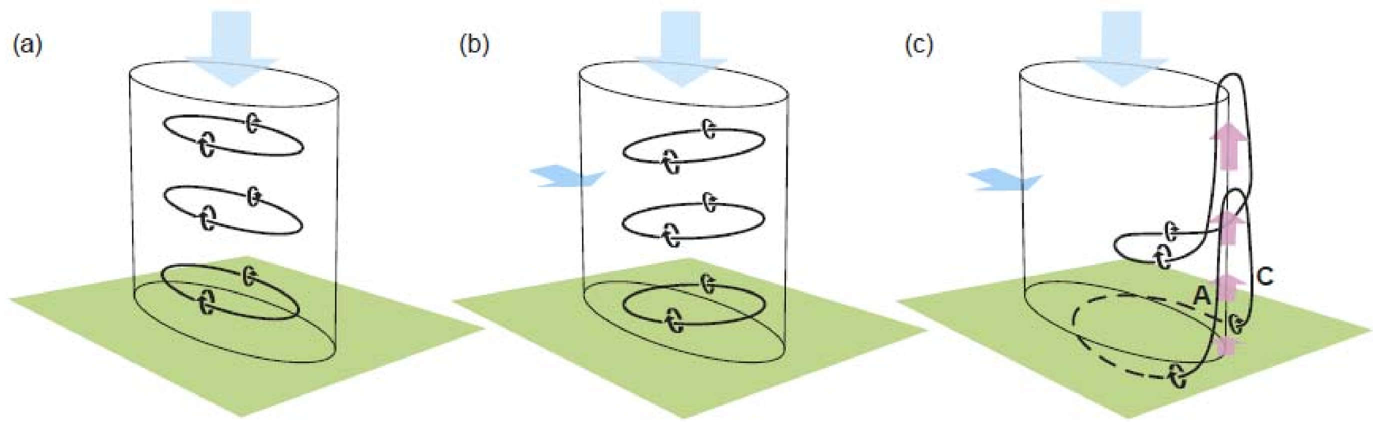

Figure 10.8 One possible way in which vertical vorticity can be produced at the surface by a purely baroclinic process in an environment containing no preexisting vertical vorticity at the surface (actually, in this idealization there is no preexisting vorticity—neither horizontal nor vertical—anywhere; the final vorticity field is solely a result of baroclinic vorticity generation and subsequent rearrangement of the baroclinically-generated vortex lines). (a) Baroclinically generated vortex rings encircle a buoyancy minimum that extends throughout a vertical column (such a region of negative buoyancy might be found in the hook echo/RFD region of a supercell, for example); the presence of negative buoyancy causes the vortex rings to sink toward the ground as they are generated. (b) If the vortex rings are swept forward as they descend toward the ground owing to the additional presence of rear-to-front flow through the buoyancy minimum, the vortex rings become tilted upward on their downstream sides (a vertical velocity gradient is present within the column because buoyancy is a minimum in the center of the column and increases with increasing distance from the center of the column). (c) If the leading edge of the vortex rings can be lifted by an updraft in close proximity to the buoyancy minimum (an updraft is typically found in close proximity to the hook echo/RFD region of a supercell, for example), then the vortex rings can be tilted further and stretched upward, leading to arching vortex lines and a couplet of cyclonic ('C') and anticyclonic ('A') vertical vorticity that straddles the buoyancy minimum and associated downdraft. (Adapted from Straka *et al.* [2007]).

Role of cold pool and baroclinic vorticity generation

- The thermal boundary is recognized as a source of low-level rotation for the tornado, through baroclinic generation of horizontal vorticity;

- However, the rain-cooled air, being negatively buoyant, resists uplift and most often surrounds the tornado, leading to its eventual demise (Figure 6a).

- It is believed that there is an optimal balance at which there is enough cool air to produce low-level rotation but not so much as to weaken the updraft and thus prevent tornado formation (Figure 6b).

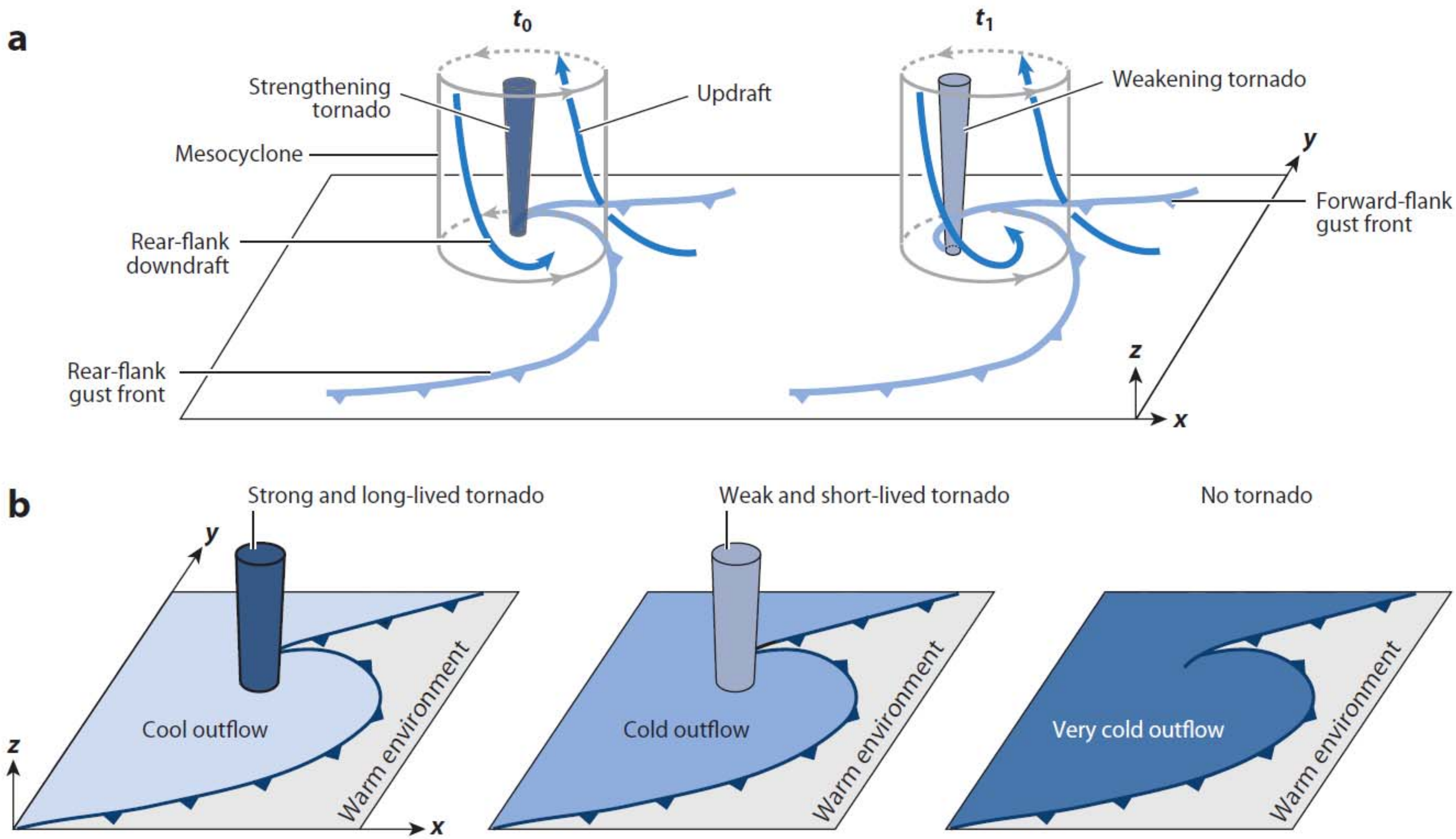

Figure 6

Illustration of a hypothesis on the effects of the cold-air boundary on tornado formation. Figure adapted from Marquis et al. (2012).

Role of surface friction and frictionally generated vorticity in tornadogenesis

Recent research has found potentially important roles of surface friction or drag in tornadogenesis.

Based detailed analysis of a numerical simulation of a real tornado case using 50-m grid spacing, Schenkman et al. (2014) found the frictionally generated horizontal vorticity as being an important contributor to the low-level rotation of tornado.

Specifically, frictionally generated low-level horizontal vorticity in the storm's inflow and outflow was found to be re-oriented into the vertical, *directly* contributing to the vertical vorticity of the tornado (**Error! Reference source not found.**). Moreover, the baroclinic mechanism was found to be largely unimportant in our analysis (**Error! Reference source not found.**b,c), especially with respect to the generation of tornadic vorticity.

Schenkman, A., M. Xue, and M. Hu, 2014: Tornadogenesis within numerically simulated 8 May 2003 Oklahoma City tornadic supercell storm. *J. Atmos. Sci.*, **71,** 130-154.

May 8th, 2003 OKC tornado

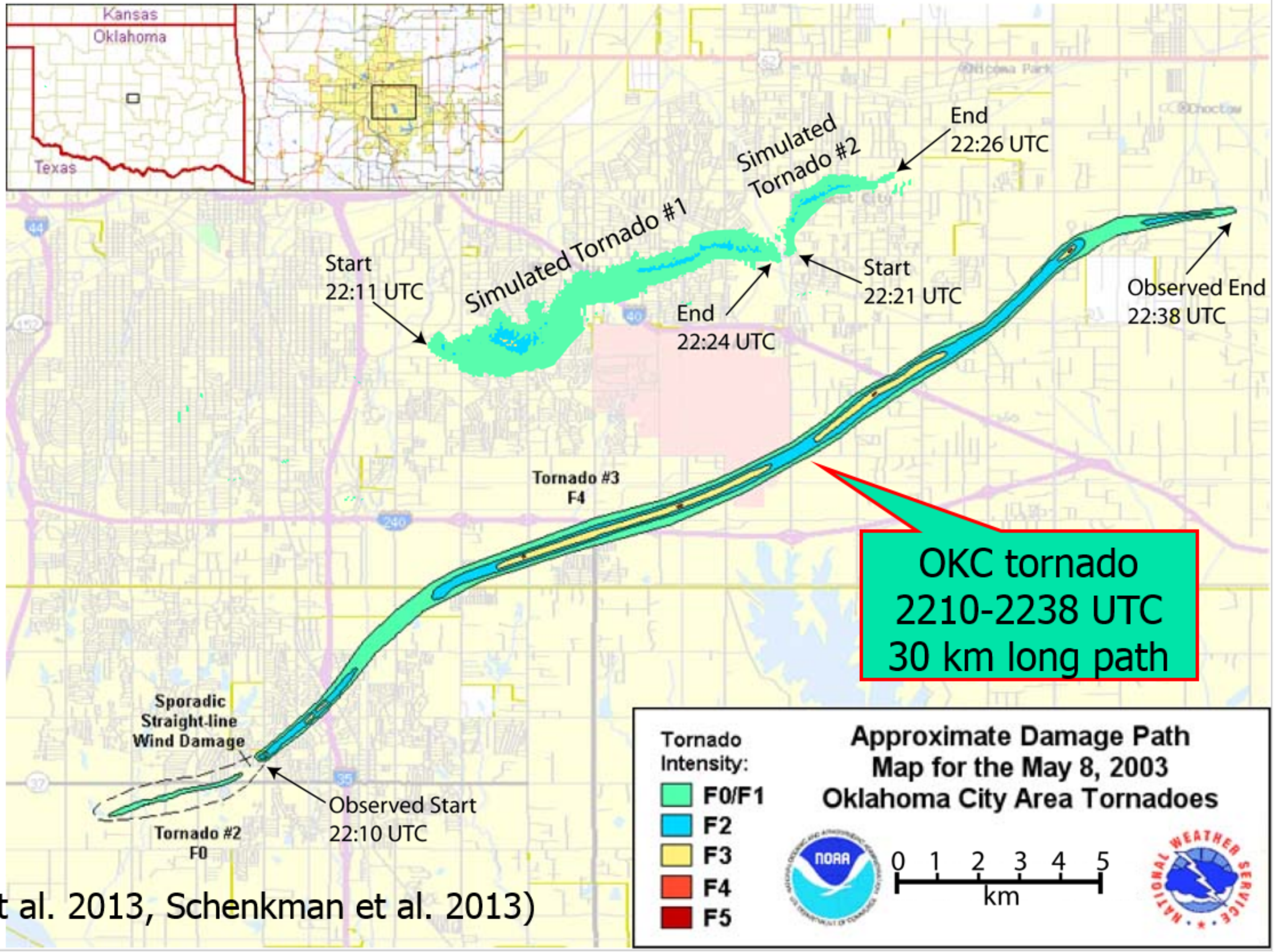

(Xue et al. 2013, Schenkman et al. 2013)

Short-Range Radar Initialized Prediction of Thunderstorms, Strong Winds, Gust Fronts, Downbursts, and Tornadoes using NWP Model

50-m Grid Forecast v.s. Observation

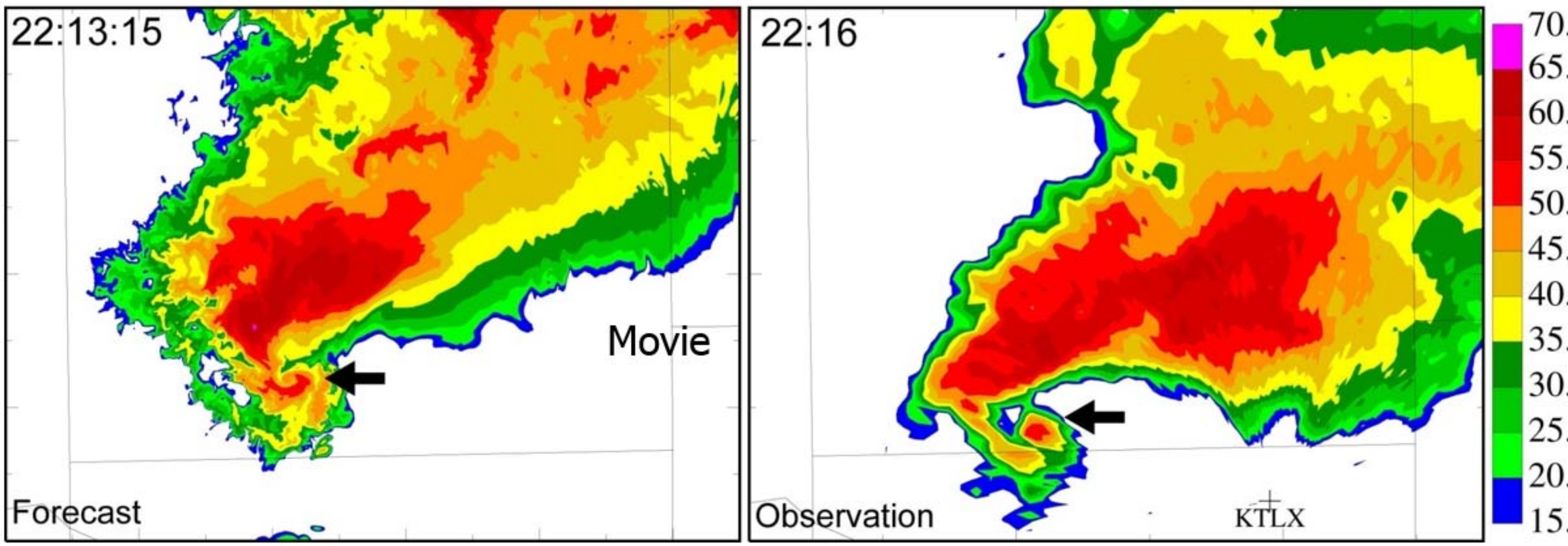

Forecast Low-level Reflectivity

Observed Low-level Reflectivity

43 minute forecast

Xue et al. (2013)

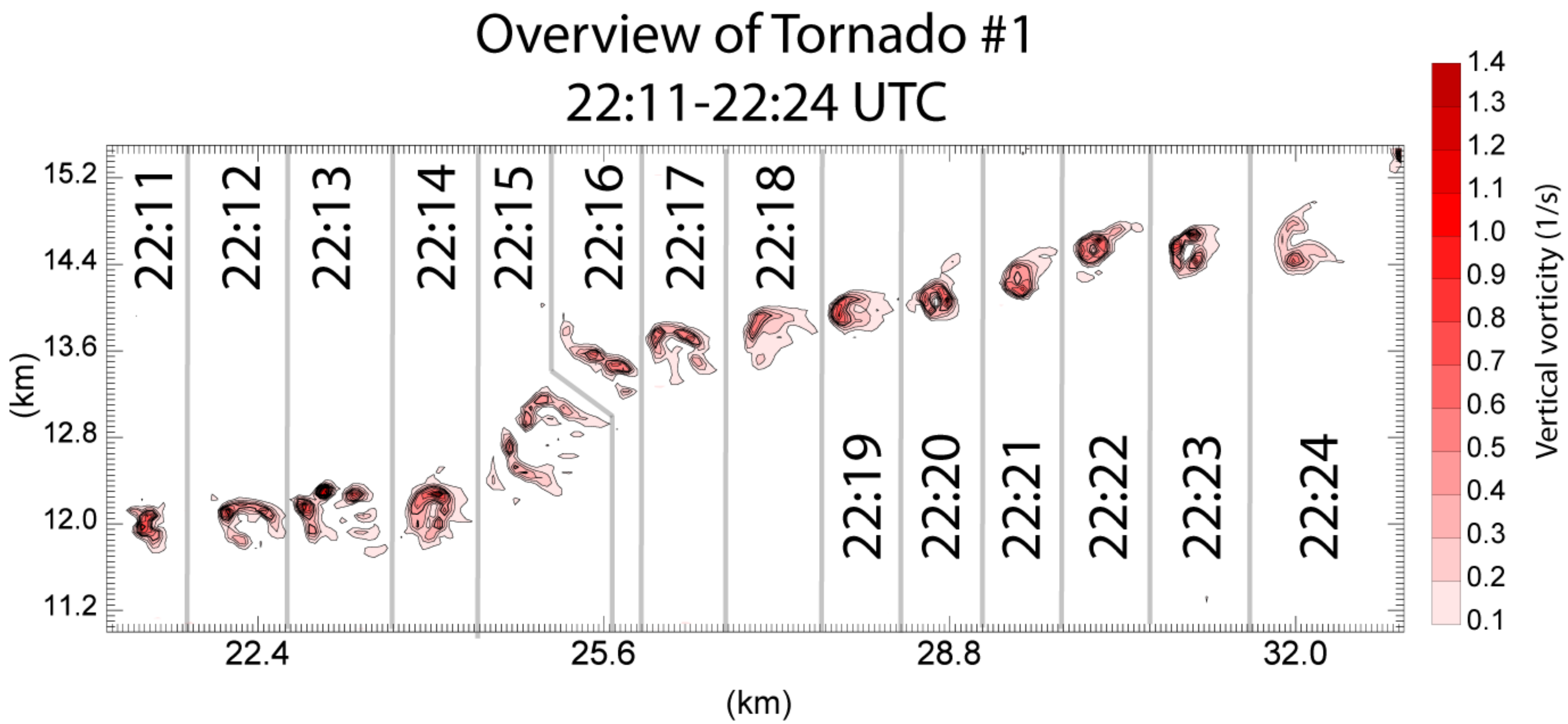
Overview of Tornado #1
22:11-22:24 UTC
22:11
22:12
22:13
22:14
22:15
22:16
22:17
22:18
22:19
22:20
22:21
22:22
22:23
22:24
15.2
14.4
13.6
12.8
12.0
11.2
(km)
22.4
25.6
28.8
32.0
(km)
Vertical vorticity (1/s)
1.4
1.3
1.2
1.1
1.0
0.9
0.8
0.7
0.6
0.5
0.4
0.3
0.2
0.1

Sfc vert. vort., and p'   E-W x-sections of vert. vort. and w

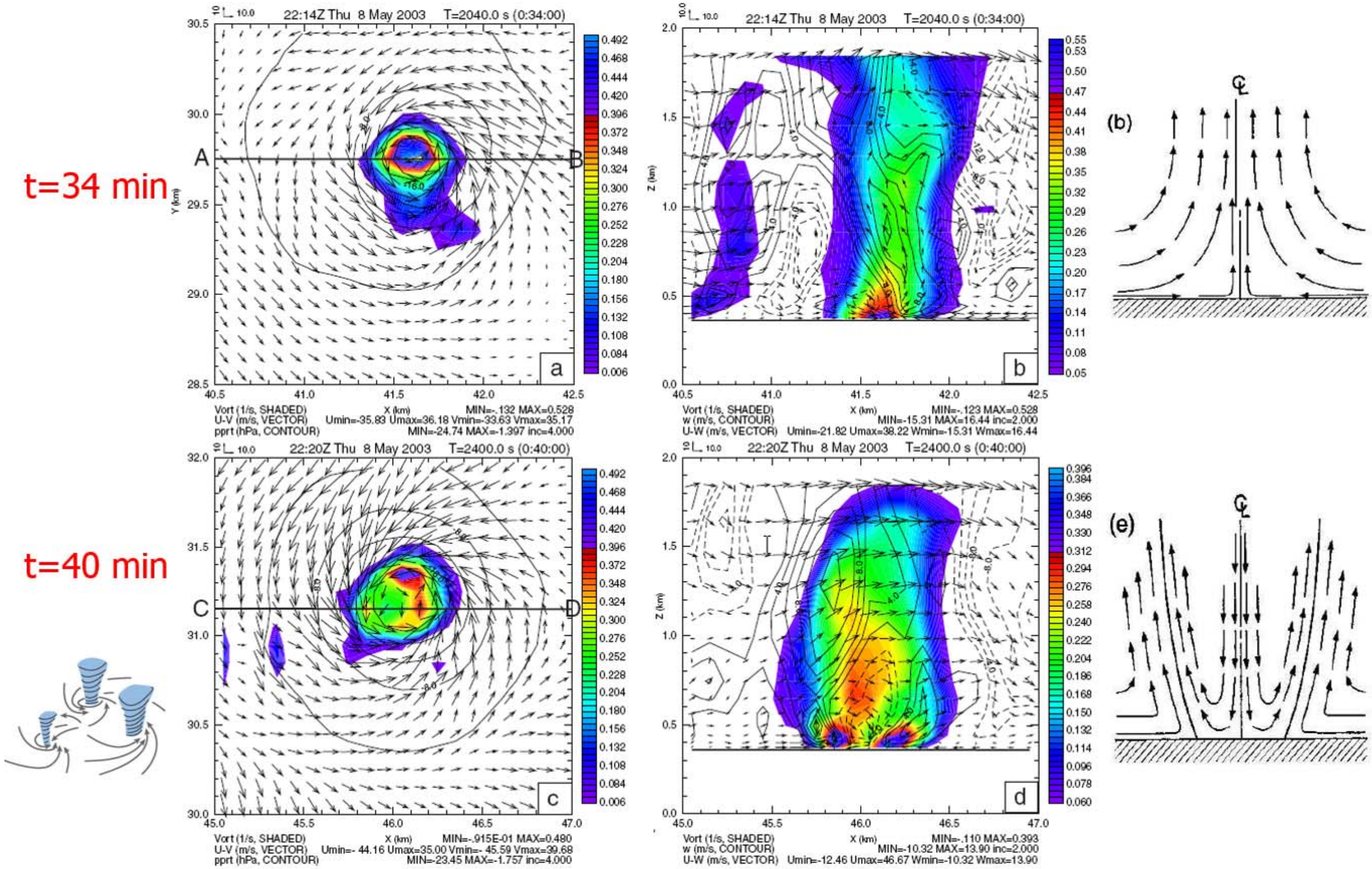

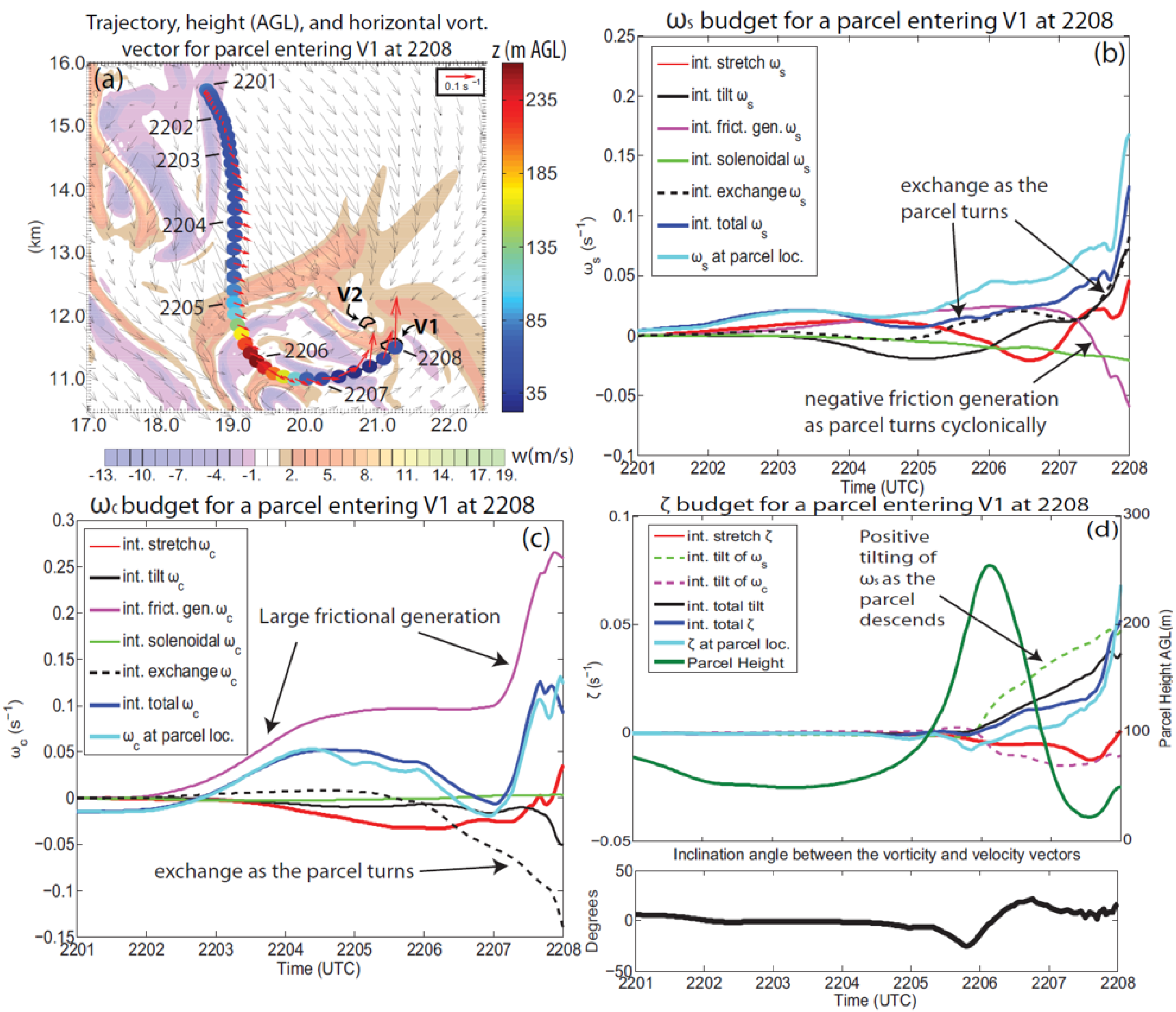

Trajectory, height (AGL), and horizontal vort. vector for parcel entering V1 at 2208
(a)
z (m AGL)
w(m/s)
V1
V2
ωs budget for a parcel entering V1 at 2208
(b)
int. stretch ωs
int. tilt ωs
int. frict. gen. ωs
int. solenoidal ωs
int. exchange ωs
int. total ωs
ωs at parcel loc.
exchange as the parcel turns
negative friction generation as parcel turns cyclonically
Time (UTC)
ωc budget for a parcel entering V1 at 2208
(c)
int. stretch ωc
int. tilt ωc
int. frict. gen. ωc
int. solenoidal ωc
int. exchange ωc
int. total ωc
ωc at parcel loc.
Large frictional generation
exchange as the parcel turns
Time (UTC)
ζ budget for a parcel entering V1 at 2208
(d)
int. stretch ζ
int. tilt of ωs
int. tilt of ωc
int. total tilt
int. total ζ
ζ at parcel loc.
Parcel Height
Positive tilting of ωs as the parcel descends
Parcel Height AGL(m)
Inclination angle between the vorticity and velocity vectors
Degrees
Time (UTC)

(a) A representative backward trajectory that terminates at 50 m AGL in an area of pre-tornadic vertical vorticity at 2208 UTC. Trajectory height (shaded circles, m AGL) and horizontal vorticity (red arrows, s^{-1}) are plotted in 10 s increments. The trajectory is overlaid on the vertical velocity (light shading, m s^{-1}) and horizontal wind (gray vectors, m s^{-1}) at 50 m AGL at 2208 UTC. Lagrangian vorticity integrations along the trajectory plotted in (a) for (b) the horizontal streamwise vorticity, (c) the horizontal crosswise vorticity, and (d) the z-component vorticity. In (b), the dark blue line is the sum of the time-integrated streamwise stretching (red line), tilting (black line), frictional generation (purple line), and baroclinic generation (green line). In (c), the dark blue line is the sum of the time-integrated crosswise stretching (red line), tilting (black line), frictional generation (purple line), and baroclinic generation (green line). In (d), the black line is the sum of the time-integrated tilting of streamwise vorticity (green dashed line) and crosswise vorticity (purple dashed line). The dark blue line in (d) is the sum of the time-integrated z-component stretching (red line) and tilting (black line). The solid green line in (d) represents the height (AGL) of the parcel. The cyan line represents the value of streamwise (in b), crosswise (in c), and z-component (in d) vorticity interpolated from the model grid to the parcel location at each time. Ideally the cyan lines match the corresponding blue lines. The inclination between the full vorticity and velocity vectors is plotted in (e). Figure reproduced from Schenkman et al. (2014).

Trajectory analysis into V2

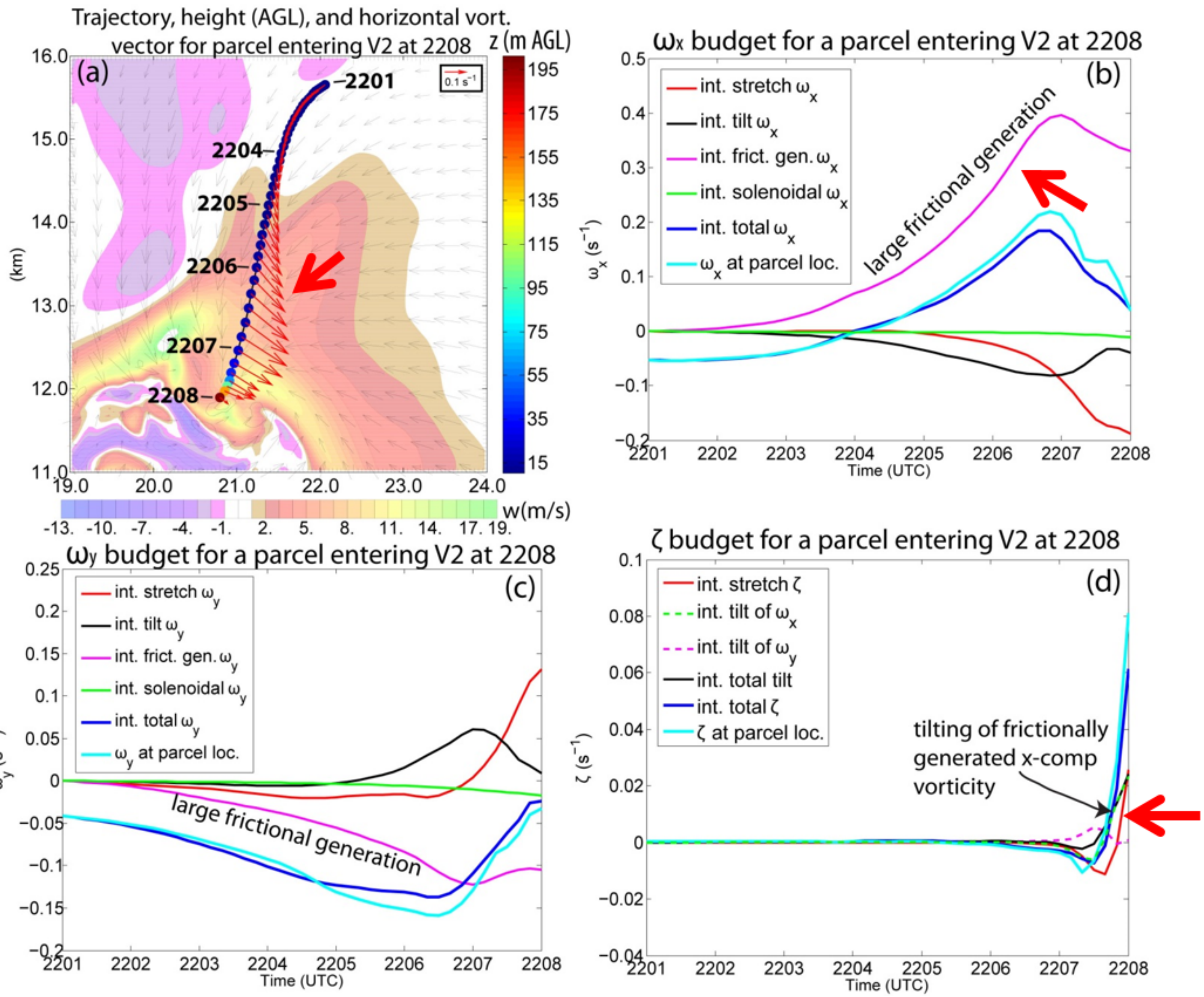

3-stage Conceptual model of Tornadogenesis
Schenkman et al. (2014)

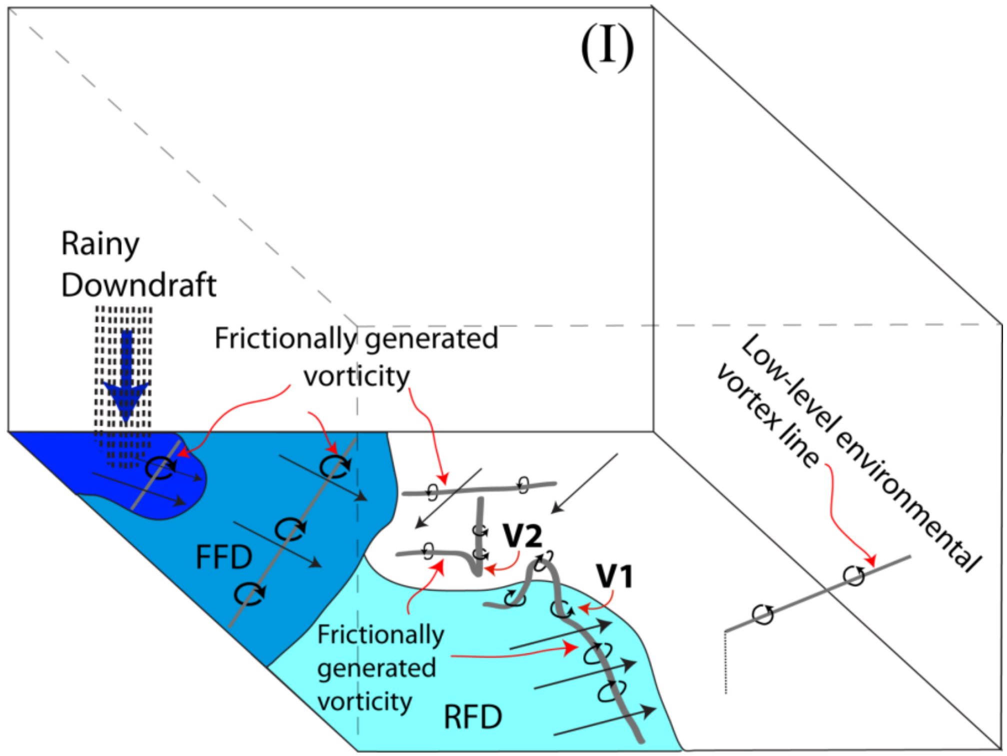

I. The RFD becomes organized with the development of a well-defined RFGF. Large, predominantly frictionally generated, vorticity develops behind the RFGF at low levels. This vorticity is tilted into the vertical as parcels descend in the northern edge of the RFGF, leading to the formation of a small vertical vorticity maximum (V1). Concurrently, large eastward-pointing horizontal vorticity is frictionally generated in low-level northerly flow behind the FFCB. As parcels are forced to rise upon encountering the RFGF, this vorticity is tilted and another small vertical vorticity maximum (V2) forms near the intersection of the RFGF and FFGF. V2 is strongest and first forms slightly above the ground.

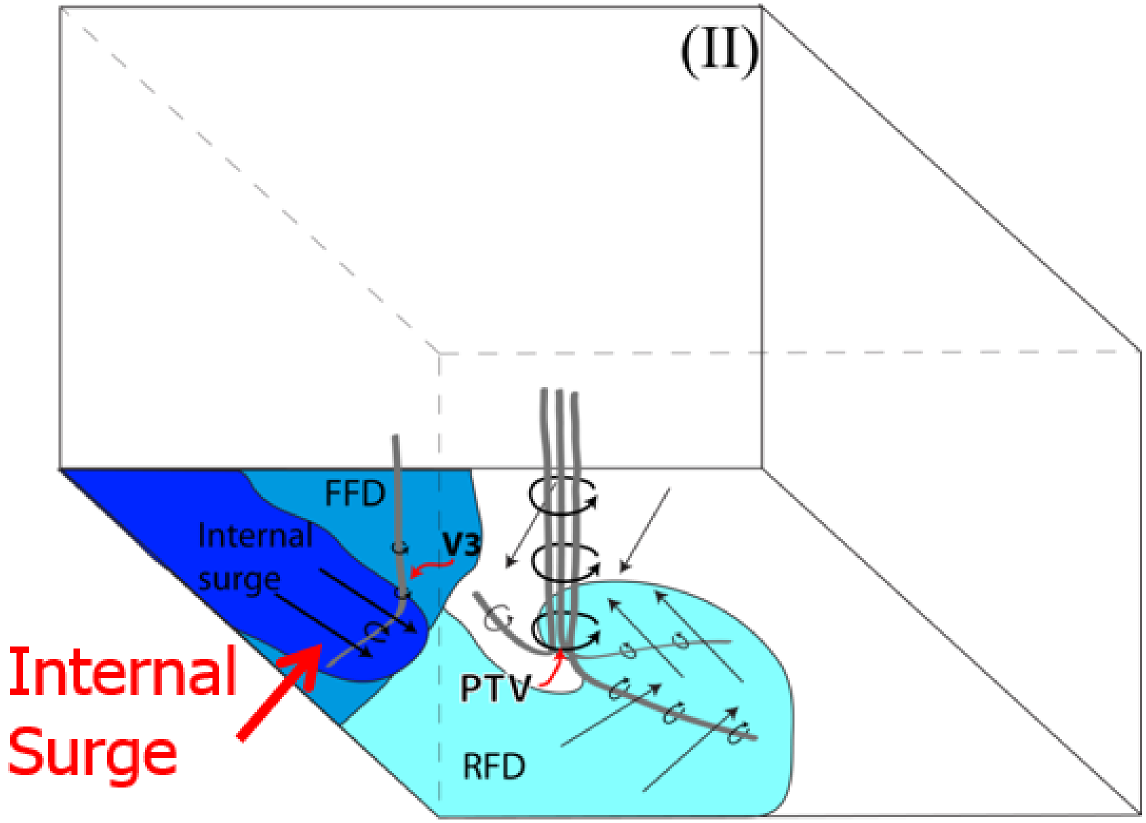

II. The two areas of vorticity described in step 1 merge to form a pre-tornadic vortex (PTV). At the same time, an internal RFD surge, that is the result of water-loading in the core of the supercell, moves quickly southeastward toward the PTV. Large northeastward-pointing horizontal vorticity is generated predominantly by surface drag at low levels within the internal RFD surge. Vertical vorticity is generated as parcels descend in the internal surge creating a third vorticity maximum (V3) on the northeast side of the internal surge (V3).

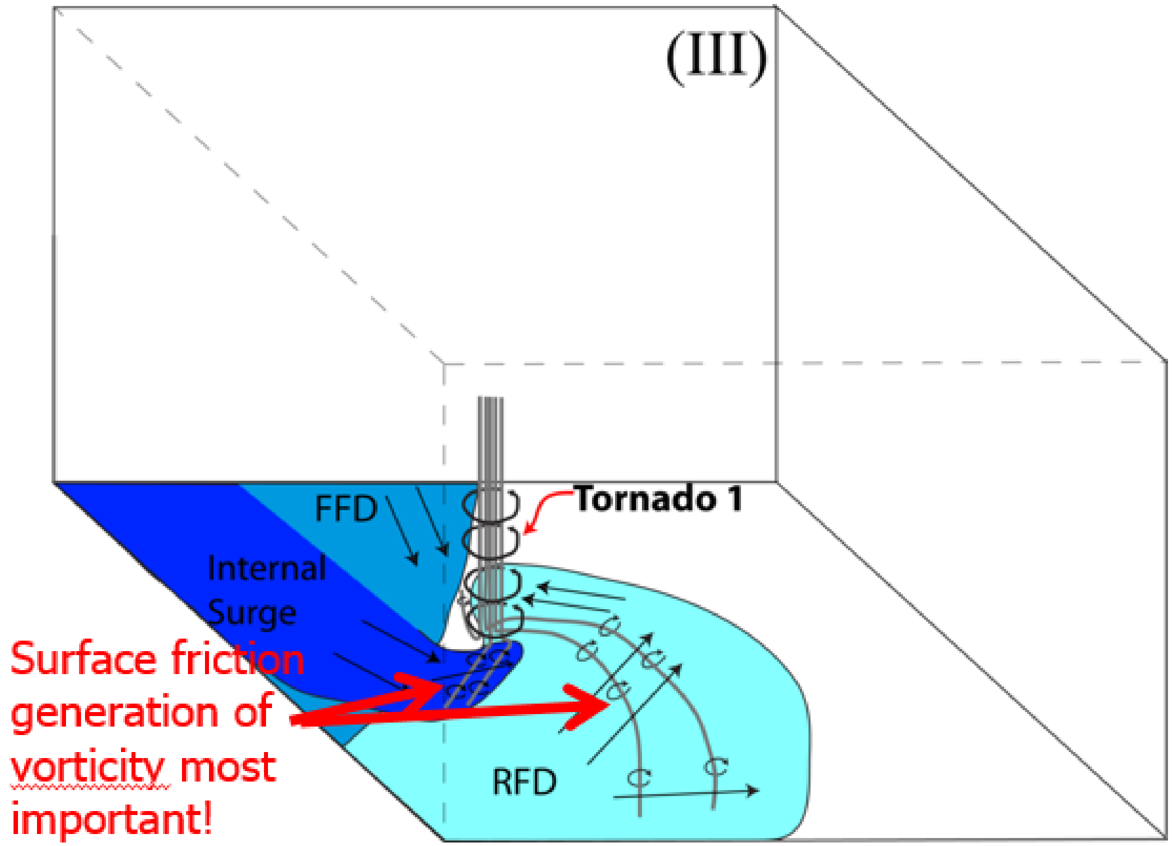

III. The internal RFD surge and the merger of V3 with the PTV trigger tornadogenesis by enhancing low-level convergence and providing a substantial source of horizontal vorticity that is readily ingested into the developing tornado.

In summary, the typical sequence of events of tornadogenesis (see good summary in Houze section 8.6):

- Storm-scale circulation and development creates the forward flank downdraft and gust front;
- The baroclinicity across the gust fronts can create horizontal vorticity that is significant larger than the environmental horizontal vorticity;
- This vorticity gets advected into the center of storm and updraft, and is tilted into vertical and stretched to intensify the vertical rotation;
- This process is believed to be responsible for the intensification of rotation at the low levels (but may not be at the ground), the lower end of the mesocyclone while the tilting of environmental vorticity is primarily responsible for the mid-level rotation/cyclone;
- The downdraft can also transport significant amount of vertical vorticity in the mid-level mesocyclone down to the surface. When this vorticity gets concentrated towards the low-level circulation center, it intensifies due to angular momentum conservation. This is believed to be at least one of the sources of ground level rotation in tornado.
- Internal outflow surges often occur, associated with enhanced downdrafts, that are either buoyancy and/or dynamic pressure driven.
- A vortex ring forms around the downdraft due to baroclinic vorticity generation, and the descent of the vortex ring with the downdraft and subsequent lifting of the vortex lines by updraft at the gust front location, and titling of the vortex lines into vertical and subsequent severe stretching is believed to be at least one of the key processes for tornadogenesis. It is believed that there is an optimal balance where the cold pool is not too cold for the cold to be difficult to lift but still cold enough to provide the baroclinic generation of vorticity.

- Another possible source of vorticity is the generation of horizontal vorticity by surface friction as downdraft air hits ground. As the air spreads at high speed along the ground, large cross-wise vorticity is generation. As the air turns cyclonically towards the developing vortex on its left side, the cross-wise vorticity becomes streamwise, and this large streamwise vorticity is tilted into vertical and stretched, leading to rapid intensification.

- Both baroclinic and friction generation of vorticity may be important for torandogensis – their relative contributions may change from case to case, and more studies are needed to understand their relative roles, as well as contributions from the environmental vorticity.

Typical Tornado Life Cycles from Observational Perspective

Read Houze section 8.8.

The tornado frequently **first becomes visible as a dust whirl on the ground under the wall cloud**.

The **condensation funnel** soon appears aloft.

Late in life, it may bend at the ground while it stretches in length and narrows in width. This final decaying stage in the tornado's life history is called the **rope stage** owing to the ropelike appearance of the condensation funnel.

The gust front associated with the RFD may tilt the tornado so that it becomes nearly horizontal.

The tornado life cycle of 10-30 min is common, but not exclusive.

For example, tornadoes sometimes occur in the absence of any condensation funnel, always look like a rope, or never go through a rope stage. Some long damage paths are associated with tornadoes that last much longer than 30 min.

Most tornadoes in supercells are cyclonic. Anticyclonic tornadoes are rare. They have been documented, however, along the RFD gust front away from the mesocyclone.

Therefore the **life cycle** can be divided into:

- **Organizing** stage – visible funnel touching ground intermittently
- **mature** stage **-** tornado reaches its full strength and damage more severe
- **shrinking** – the funnel decreases to a thin column
- **decay** stage – funnel becomes fragments, contorted and still destructive

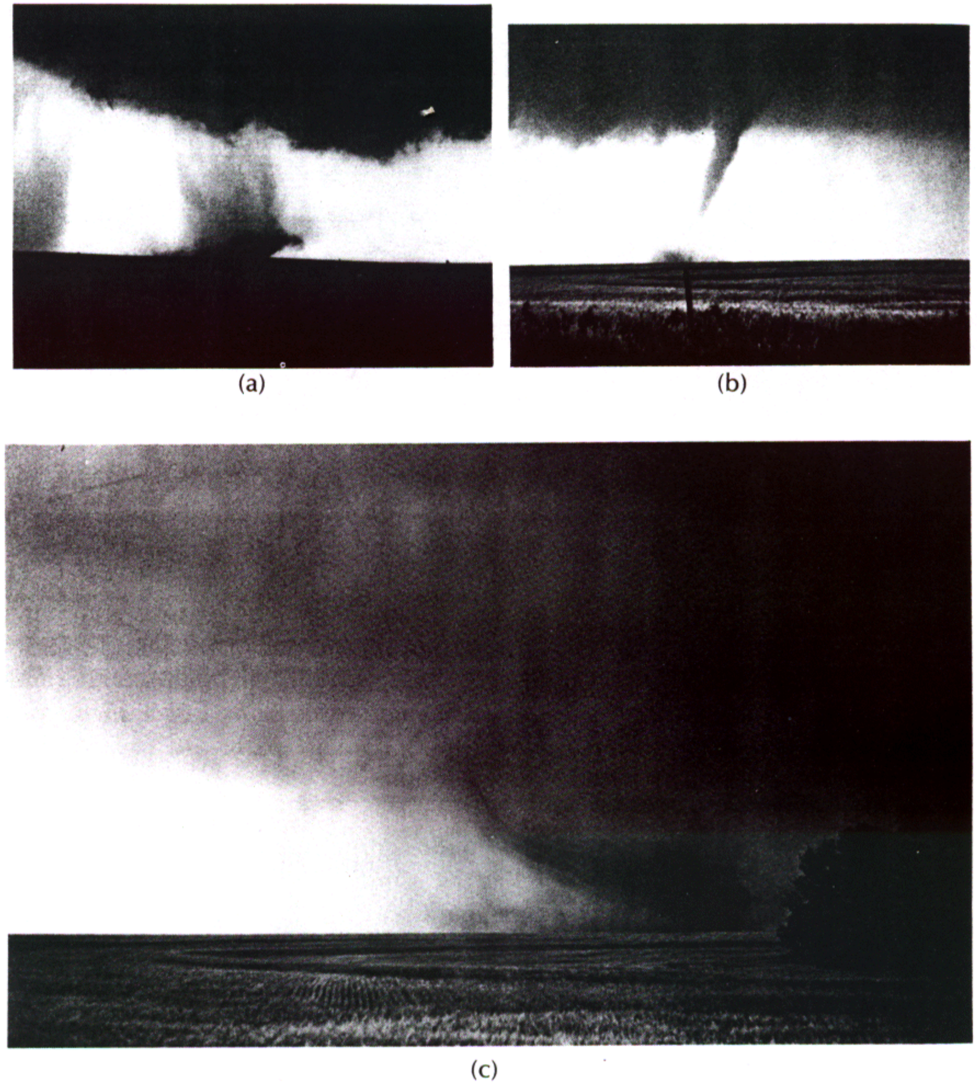

Figure 3.46 A series of photographs depicting the life cycle of a tornado: (a) a dust whirl appears near the ground, underneath the wall cloud; (b) a condensation funnel builds downward from cloud base; (c) the tornado becomes tilted and stretches out just before it dissipates (from Bluestein, 1983). This tornado occurred near Cordell, Oklahoma on May 22, 1981 (photographs copyright H. Bluestein). [(c) courtesy of the American Meteorological Society]

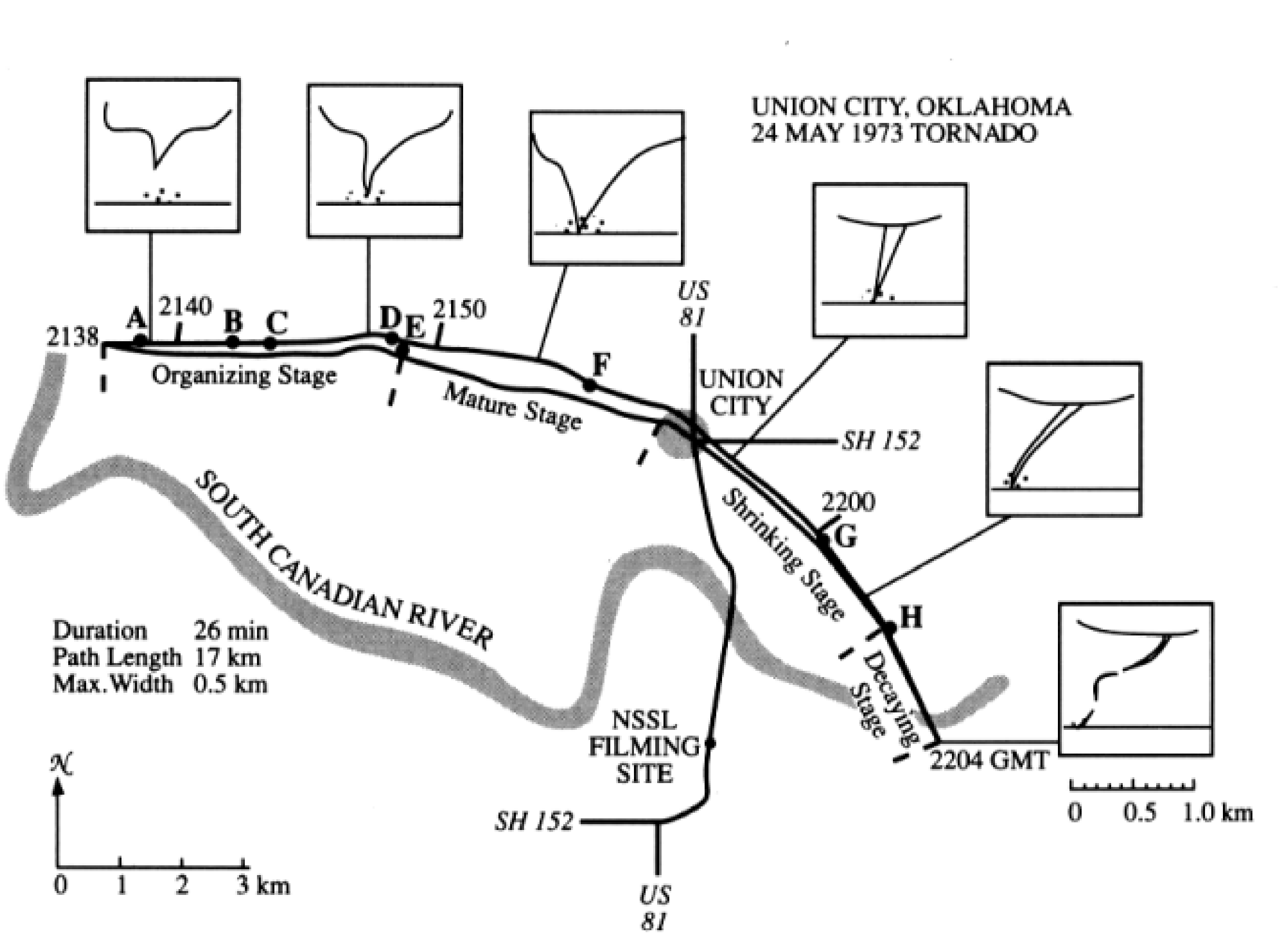

Figure. Structure of a tornado observed at several stages of its life cycle. Sketches show funnel cloud and associated debris.

<u>Multi-vortex tornadoes</u>

Although tornadoes frequently consist of a single vortex, they occasionally exist as two or more smaller "**suction vortices**" that rotate around the center of the wall cloud.

Laboratory model and numerical model evidence suggests that **multiple vortices are associated with high "swirl ratio**," that is, relatively large azimuthal flow compared to radial flow.

Suction vortices often have a lifetime of only one revolution around the wall cloud; new ones form and dissipate in the identical location relative to the mesocyclone.

Sometimes **multiple-vortex tornadoes evolve into single-vortex tornadoes, and vice versa**.

Some suction vortices extend all the way to cloud base; others are visible only near the ground underneath a broader rotating cloud base.

The multiple-vortex phenomenon was first postulated by T. Fujita on the basis of cycloidal damage swaths.

The **"suction vortices" create greater maximum wind speed** inside the tornadoes vortex because the effect due to the smaller and larger vortices are additive. They are observed to be particularly dangerous and damaging.

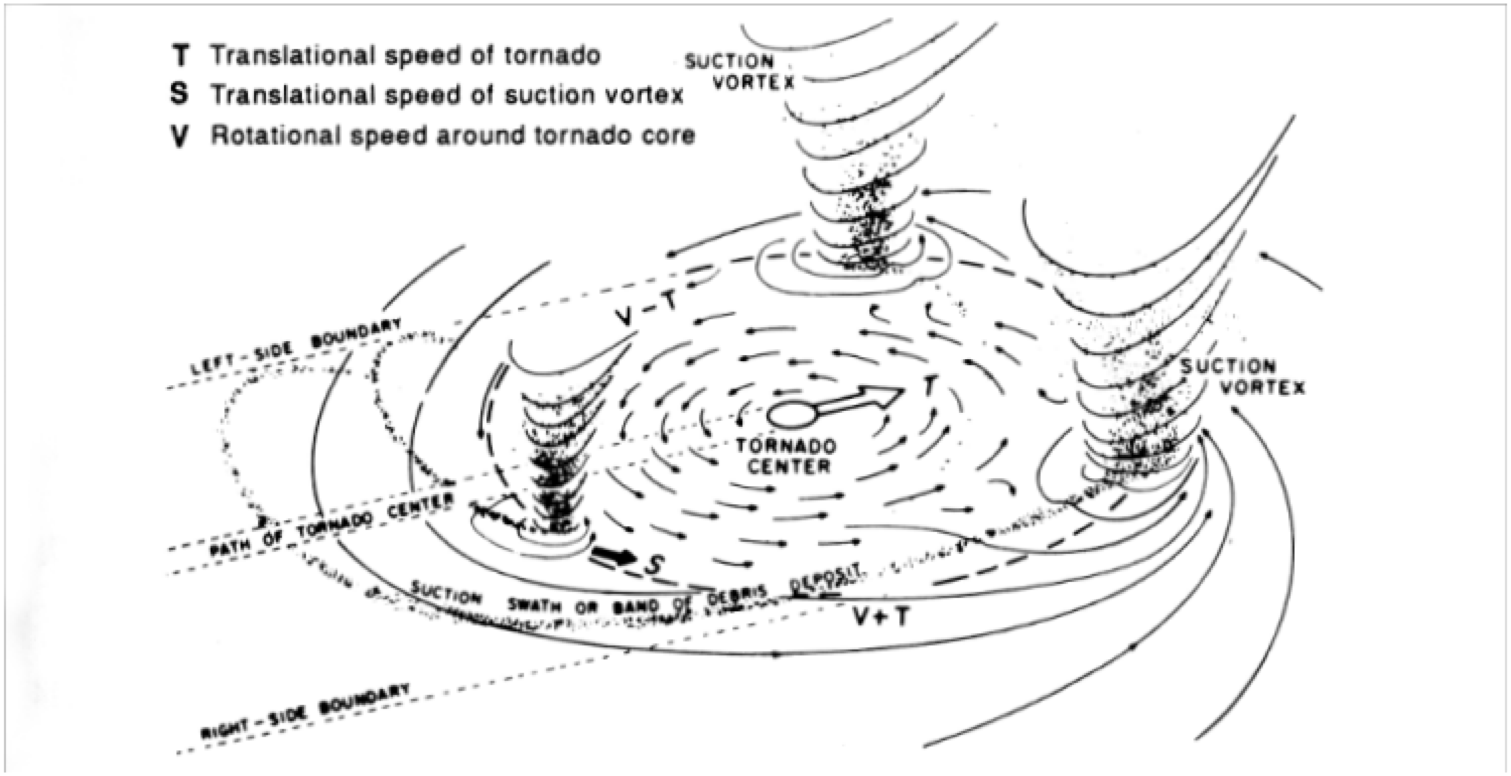
T Translational speed of tornado
S Translational speed of suction vortex
V Rotational speed around tornado core
SUCTION VORTEX
SUCTION VORTEX
V-T
T
TORNADO CENTER
LEFT-SIDE BOUNDARY
PATH OF TORNADO CENTER
S
SUCTION SWATH OR BAND OF DEBRIS DEPOSIT
V+T
RIGHT-SIDE BOUNDARY

Figure 4

An example of a multiple-vortex tornado. Photograph courtesy of H.B. Bluestein.

Different forms of tornado vortex

Based on laboratory vortex studies that are confirmed by numerical simulations, a parameter called swirl ratio ($S = r_0\Gamma_s /(2Q)$, where Γ_s is the angular rotation rate) to a large extent determine the form of tornado vortex.

1. For low values of S, the flow takes the form of a single vortex in an updraft extending from the surface through the depth of the chamber (**Figure 9*a***).
2. At somewhat larger values of S, the single vortex in an updraft undergoes a transition at some level above the surface to a single vortex with a central downdraft surrounded by updraft (**Figure 9*b***).
3. For larger values yet of S, the central downdraft penetrates to the lower surface (**Figure 9*c***).
4. Finally, at the largest values of S, the single two-celled vortex undergoes a transition to multiple vortices revolving about a common center (**Figure 9*d***).

Some real tornadoes go through all four stages as it intensifies then weakens as axial downdraft develops.

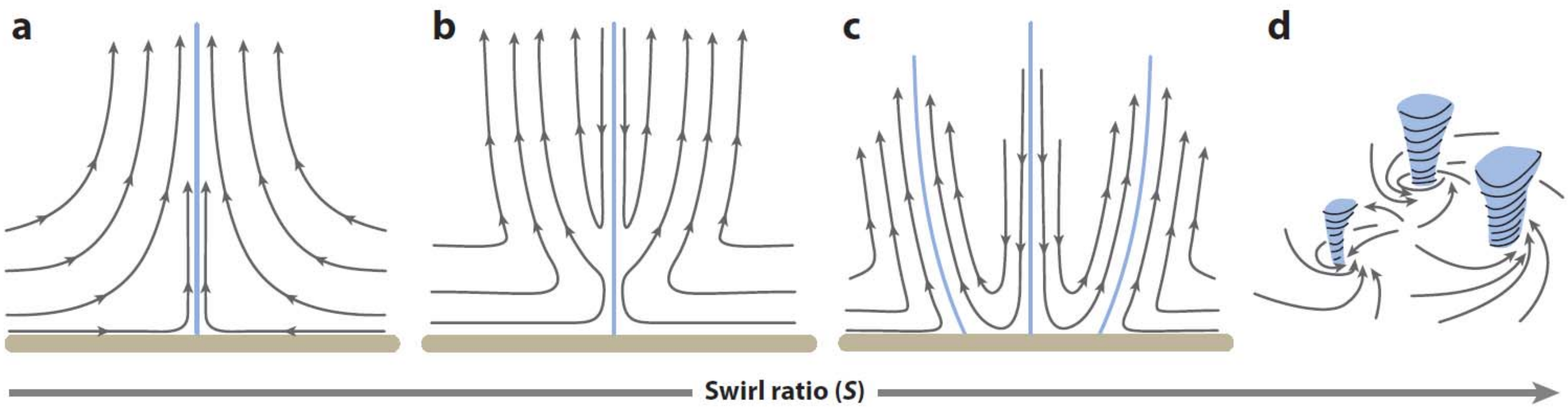

Figure 9

For increasing swirl ratio, S, Ward (1972) showed that the form of the vortex changes from (*a*) single-celled to (*b*) single-celled below and doubled-celled above to (*c*) doubled-celled to (*d*) multiple vortices. Figure adapted from Davies-Jones (1986).

Nonsupercell tornadoes and Gustnadoes

Read Houze section 8.7.

Tornadoes don't occur exclusively in supercells.

Non-supercell tornadoes can occur along a low-level convergence line underneath growing cumulus clouds.

Preexisting vortices along the line get stretched in the vertical by updraft of the growing cumulus cloud and intensify to form usually relative weak tornadoes.

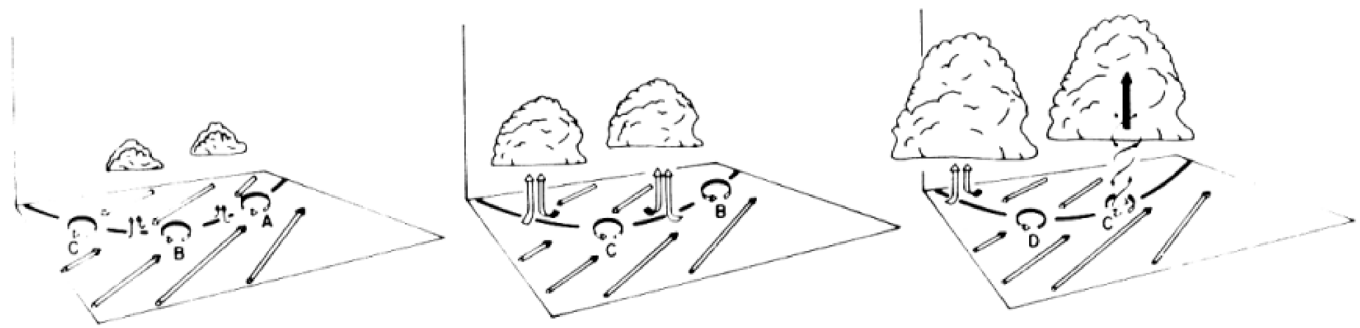

Figure 3.49 Schematic model of the life cycle of the nonsupercell tornado. The black line is the radar detectable convergence boundary. Low-level vortices are labeled with letters. At the left, clouds begin to form over the convergence zone, along which there are pre-existing vortices. In the middle, strong updrafts develop beneath the growing cumulus congestus clouds. At the right, a strong updraft becomes superimposed on one of the pre-existing vortices, and a tornado forms. The tornado dissipates when precipitation falls out of the updraft and the cell collapses (from Wakimoto and Wilson, 1989). (Courtesy of the American Meteorological Society)

Lee and Wilhemson (1997) present a very nice numerical study on nonsupercell tornadogenesis. The following figure is taken from the paper:

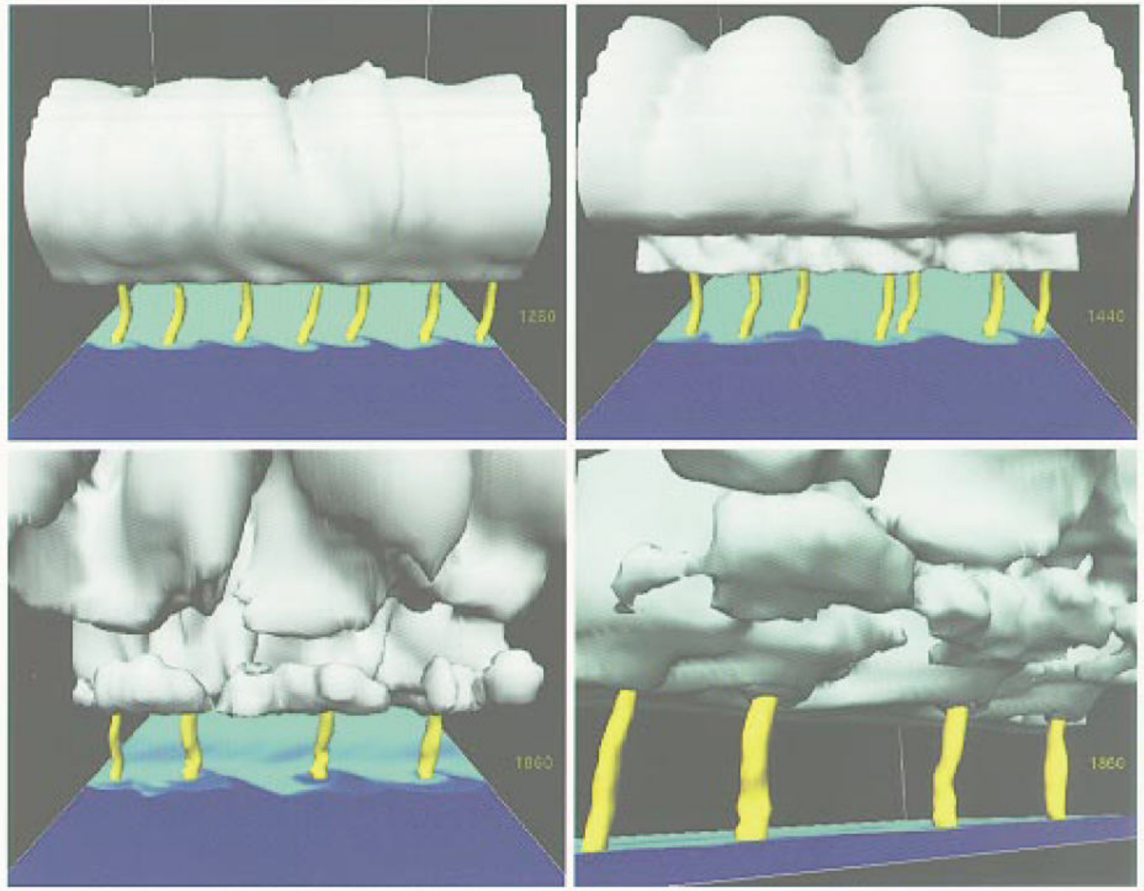

FIG. 4. Three-dimensional model renderings of the evolving ensemble of leading edge vortices, storm, and outflow boundary for 1260, 1440, and 1860 s. At the domain base the blue color spectrum delineates the outflow boundary (darker = colder). The yellow vertical vortex tubes are representative of vertical vorticity greater than 0.1 s^{-1}. The gray-scaled cloud isosurface represents cloud water greater than 0.2 g kg^{-1}. Viewing perspective in the first three panels is from an elevated position looking east, while the viewing position in the fourth panel is surface-based, looking southeast.

Reference: Lee, B. D. and R. B. Wilhelmson, 1997: The Numerical Simulation of Nonsupercell Tornadogenesis. Part II: Evolution of a Family of Tornadoes along a Weak Outflow Boundary. *J. Atmos. Sci.*, **54,** 2387-2415.

Low-level convergence helps concentrate the vertical vorticity.

The vortex intensification can be further aided by rotation in the convective updraft.

Gustnadoes are short lived vortices occurring along preexisting gust fronts, coming into existence mainly due to horizontal shear instability.

Waterspouts: Vortices forming over water often along outflow boundaries of nearby shower. The processes involved are similar to the land-based non-supercell tornadoes forming along a gust front.